A nitrogen response pathway regulates virulence functions in *Fusarium oxysporum* via the protein kinase TOR and the bZIP protein MeaB

Manuel S. López-Berges, Nicolas Rispail, Rafael C. Prados-Rosales and Antonio Di Pietro[1]

Departamento de Genética, Universidad de Córdoba, Campus de Rabanales Edificio Gregor Mendel, 14071 Córdoba, Spain

Running title: Nitrogen regulates virulence in *Fusarium*

Estimated length of published article: 14.5 pages

[1]Address correspondence to ge2dipia@uco.es.
The author responsible for distribution of materials integral to the findings presented in this article in accordance with the policy described in the Instructions for Authors (www.plantcell.org) is: Antonio Di Pietro (ge2dipia@uco.es).

Synopsis: Nitrogen limitation was proposed to act as a signal for infectious development in plant pathogens. Here we show that the preferred nitrogen source ammonium represses a set virulence-related functions in the vascular wilt fungus *Fusarium oxysporum*, and identify two key elements of the nitrogen response pathway, the conserved protein kinase TOR and the bZIP factor MeaB.

ABSTRACT

During infection, fungal pathogens activate virulence mechanisms such as host adhesion, penetration and invasive growth. In the vascular wilt fungus *Fusarium oxysporum* the mitogen-activated protein kinase Fmk1 is required for plant infection and controls processes such as cellophane penetration, vegetative hyphal fusion or root adhesion. Here we show that these virulence-related functions are repressed by the preferred nitrogen source ammonium, and restored by treatment with L-methionine sulfoximine (MSX) or rapamycin, two specific inhibitors of glutamine synthetase and the protein kinase TOR, respectively. Deletion of the bZIP protein MeaB also resulted in nitrogen source independent activation of virulence mechanisms. Activation of these functions did not require the global nitrogen regulator AreA, suggesting that MeaB-mediated repression of virulence functions does not act through inhibition of AreA. Tomato plants supplied with ammonium rather than nitrate showed a significant reduction in vascular wilt symptoms when infected with the wild type but not with the Δ*meaB* strain. Nitrogen source also affected invasive growth in the rice blast fungus *Magnaporthe oryzae* and the wheat head blight pathogen *F. graminearum.* We propose that a conserved nitrogen responsive pathway might operate via TOR and MeaB to control virulence in plant pathogenic fungi.

INTRODUCTION

Plant pathogenic fungi have evolved mechanisms to invade their hosts, overcome their defences and colonize their tissues, thereby causing disease. Expression of these virulence functions is controlled by a network of cellular pathways that respond to signals encountered during host infection. A conserved mitogen activated protein kinase (MAPK) cascade homologous to the yeast mating and filamentation cascade is essental for pathogenicity in a wide range of plant pathogens (Xu and Hamer, 1996; Zhao et al., 2007). The orthologous MAPK Fmk1 is required for plant infection in the vascular wilt fungus *Fusarium oxysporum*, a soilborne pathogen that attacks a wide range of economically important crops (Di Pietro et al., 2001). *F. oxysporum* mutants lacking *fmk1* are impaired in multiple virulence-related processes such as root adhesion, host penetration and invasive growth on the living plant tissue (Di Pietro et al., 2001). Fmk1 is also required for vegetative hyphal fusion, an ubiquitous developmental process in filamentous fungi (Prados Rosales and Di Pietro, 2008). The cellular mechanisms through which this conserved MAPK cascade controls such a wide array of pathogenicity mechanisms are largely unknown.

Nitrogen limitation has been proposed as a key signal for activating the expression of virulence genes in plant pathogens (Snoeijers et al., 2000). Early studies established that *in planta* induced genes such as *mpg1* encoding a hydrophobin required for pathogenicity of the rice blast fungus *Magnaporthe oryzae*, or the avirulence gene *avr9* of the tomato pathogen *Cladosporium fulvum*, are strongly upregulated under conditions of nitrogen limitation (Talbot et al., 1993; Van den Ackerveken et al., 1994). In agreement with these findings, many genes identified in screens for nitrogen starvation-induced transcripts are also upregulated during plant infection (Coleman et al., 1997; Stephenson et al., 1997; Divon et al., 2005; Donofrio et al., 2006). Thus, nitrogen source seems to act as a metabolic switch to trigger expression of infection-related genes in plant pathogenic fungi.

Nitrogen utilization is a highly regulated process. Although fungi are able to use a wide variety of nitrogen sources, readily assimilated compounds such as ammonium or glutamine are used preferentially over more complex sources

(Marzluf, 1997). This is accomplished by a process known as nitrogen catabolite repression, whereby genes required for exogenous nitrogen source utilization are downregulated in the presence of the preferred source (Marzluf, 1997; Wong et al., 2008). Transcriptional regulation of nitrogen catabolic genes is mediated, in part, by the wide-domain regulators AreA in *Aspergillus nidulans* (Arst and Cove, 1973), Nit-2 in *Neurospora crassa* (Fu and Marzluf, 1987) and Gln3/Gat1 in *Saccharomyces cerevisiae* (Beck and Hall, 1999). These global nitrogen regulators are members of the GATA family of DNA binding proteins, and function as transcriptional activators of genes encoding pathway-specific permeases and enzymes enabling uptake and catabolism of secondary nitrogen sources (Caddick et al., 1986; Fu and Marzluf, 1990). As a consequence, loss-of-function mutants in *areA* or *nit-2* are unable to utilize nitrogen sources other than glutamine or ammonium (Arst and Cove, 1973; Marzluf, 1997). AreA orthologues have been identified in a number of filamentous ascomycetes and appear to be both structurally and functionally conserved (Wong et al., 2008).

Since AreA regulates gene expression under nitrogen-limiting conditions similar to those encountered *in planta*, its role in expression of virulence genes and in disease development has been examined in several plant pathogens. The AreA orthologue from *C. fulvum,* NRF1, partly controlled expression of *avr9*, but *nrf1* mutants still produced low levels of *avr9* transcript *in planta* and were fully virulent (Perez-Garcia et al., 2001). Similarly, NUT1, the AreA orthologue of *M. oryzae,* was required for full induction of *MPG1* expression (Soanes et al., 2002) but not for pathogenicity on rice plants (Froeliger and Carpenter, 1996). In other plant pathogens such as *Colletotrichum lindemuthianum* or *F. oxysporum*, inactivation of *areA* orthologues decreased virulence to different degrees (Pellier et al., 2003; Divon et al., 2006). Collectively, these studies suggest that AreA contributes to, but is not essential for fungal virulence on plants.

Interestingly, a genetic screen for nitrogen non-utilizing mutants in *M. oryzae* identified mutations in two genes that were non-allelic to *NUT1* and dramatically affected pathogenicity. These mutants failed to utilize a range of nitrogen sources and were non-pathogenic on rice (Lau and Hamer, 1996), suggesting a major role of nitrogen regulation in plant infection which appears to be largely

independent of AreA. The identity of these nitrogen responsive virulence regulators has not been elucidated so far.

The conserved serine/threonine kinase TOR (Target Of Rapamycin) orchestrates cell growth in eukaryotes in response to nutrient availability (De Virgilio and Loewith, 2006; Rohde et al., 2008). In *S. cerevisiae,* inhibition of TOR by rapamycin causes a nutrient stress response, including inhibition of translation initiation, arrest in the G1 phase of the cell cycle, glycogen accumulation, downregulation of glycolysis, and autophagy (Crespo and Hall, 2002). Nitrogen is a particularly important nutrient in TOR signaling. Both nitrogen starvation and rapamycin resulted in rapid dephosphorylation and nuclear accumulation of Gln3, followed by expression of genes involved in the assimilation of alternative nitrogen sources (Beck and Hall, 1999; Crespo and Hall, 2002). Depletion of the preferred nitrogen source glutamine by treatment with the glutamine synthetase inhibitor L-methionine sulfoximine (MSX) also caused nuclear localization of Gln3p, suggesting that TOR responds to glutamine levels (Crespo et al., 2002). In the filamentous fungus *Fusarium fujikuroi*, TOR inhibition by rapamycin affected expression of AreA-controlled genes involved in secondary metabolism, translation control, ribosome biogenesis, carbon metabolism and autophagy (Teichert et al., 2006). The role of TOR in nutrient regulation of fungal virulence on plants has not been examined so far.

The present study was initiated with the aim to explore a possible crosstalk between nitrogen signalling and the Fmk1 MAPK cascade in the control of virulence functions of *F. oxysporum*. The initial hypothesis was based on the finding that in *S. cerevisiae,* invasive pseudohyphal growth requires both nitrogen limitation and the orthologous Kss1 MAPK cascade (Gimeno et al., 1992; Madhani and Fink, 1997). We previously noted that cellophane penetration, a virulence-related process with analogies to agar invasion in yeast, requires the MAPK Fmk1 and the downstream homeodomain transcription factor Ste12 (Prados Rosales and Di Pietro, 2008; Rispail and Di Pietro, 2009). Here we show that the preferred nitrogen source ammonium represses cellophane penetration in *F. oxysporum* and other plant pathogenic fungi, and that this repression is reversed by inhibition of glutamine synthetase or TOR by MSX and rapamycin, respectively. Nitrogen source and TOR control

additional virulence-related functions such as vegetative hyphal fusion and root adhesion. We further establish that repression of virulence functions by ammonium requires the bZIP protein MeaB. Finally, we show that nitrogen source and MeaB control expression of virulence-related genes during *F. oxysporum* infection and production of vascular wilt disease on tomato plants. We propose the existence of a conserved nitrogen response pathway that operates via TOR and MeaB to negatively regulate virulence functions in plant pathogenic fungi.

RESULTS

Nitrogen source regulates cellophane penetration in plant pathogenic fungi

We previously found that the ability of *F. oxysporum* to cross cellophane membranes defines a major virulence function that requires the Fmk1 MAPK cascade (Prados Rosales and Di Pietro, 2008; Rispail and Di Pietro, 2009). In order to investigate the role of nitrogen regulation in this process, we determined cellophane invasion of the *F. oxysporum* wild type strain on minimal medium supplemented with different nitrogen sources. Efficient penetration was detected on sodium nitrate, but not on ammonium nitrate, ammonium sulphate or ammonium tartrate, suggesting an inhibitory effect of the preferential nitrogen source ammonium (Figure 1A). Penetration on nitrate was largely independent of carbon source, since it occurred both on glycerol and on the preferred carbon source glucose at concentrations as high as 5% (w/v) (Supplemental Figure 1A online). However, glucose limitation (0.2%) partially relieved inhibition of cellophane penetration by ammonium (Supplemental Figure 1B online).

We investigated whether the repressing effect of ammonium was functional in other plant pathogenic fungi by testing cellophane penetration in two ascomycete pathogens that differ from *F. oxysporum* in host range and mode of infection. The head blight pathogen *F. graminearum* infects developing spikes of wheat and barley (Jansen et al., 2005), while the rice blast fungus *M. oryzae* penetrates rice leaves by means of specialized dome shaped appressoria

(Talbot, 2003). *F. graminearum* isolate PH-1 and *M. oryzae* isolate Guy-11 both were able to cross cellophane membranes when grown on sodium nitrate, but not on ammonium nitrate (Figure 1B). These results indicate that inhibition of cellophane penetration by ammonium is conserved in these plant pathogenic ascomycetes.

Nitrogen repression of invasive growth requires glutamine synthetase and TOR

Among the different amino acids tested as nitrogen sources, only glutamine partially repressed cellophane penetration (Table 1). Repression by glutamine was less efficient than by ammonium, possibly due to the inherent instability or inefficient uptake of this amino acid (Figure 2B). We therefore used MSX, an irreversible and highly specific inhibitor of glutamine synthetase (Crespo et al., 2002) (Figure 2A), to further investigate the role of glutamine in nitrogen repression. MSX fully restored cellophane penetration of *F. oxysporum* on ammonium (Figure 2B). Thus, glutamine synthetase activity is strictly required for ammonium-mediated inhibition of cellophane penetration, suggesting that glutamine rather than ammonium acts as a signal for nitrogen repression.

In *S. cerevisiae,* intracellular glutamine levels regulate the activity of the conserved protein kinase TOR (Crespo and Hall, 2002; Crespo et al., 2002) (Figure 2A). In contrast to *S. cerevisiae* which has two TOR proteins, only a single TOR orthologue was identified in filamentous ascomycetes such as *A. nidulans*, *F. fujikuroi* and *Podospora anserina* (Dementhon et al., 2003; Fitzgibbon et al., 2005; Teichert et al., 2006). Unexpectedly, a Blastp analysis of the *Fusarium* comparative genome database detected two *tor* gene orthologues in *F. oxysporum*, *FOXG_02818* and *FOXG_15946*, compared to a single orthologue in the closely related species *F. graminearum* and *F. verticillioides*. The *FOXG_02818* gene is located on chromosome 8 and encodes a full length TOR protein (named TOR1a), while *FOXG_15946* is on chromosome 2b and encodes a truncated TOR orthologue (TOR1b) which lacks the 633 N-terminal amino acid residues and has 93% amino acid identity to *FOXG_02818* in the remaining part of the protein. Approximately 8 kb upstream of *FOXG_15946,* a

short open reading frame (ORF) *FOXG_15944* encodes 399 N-terminal amino acids of TOR, and is separated from *FOXG_15946* by an gene with homology to helitron-like transposons (Poulter et al., 2003). The predicted *tor1b* gene product contains 3 of the 4 N-terminal HEAT repeats, as well as all the other key domains of TOR proteins. RT-PCR analysis with primer pairs specific for each of the *tor* genes detected abundant transcript levels of *tor1a* and a very faint signal corresponding to the *tor1b* transcript (Supplemental Figure 2 online). This result suggests that the two *tor* genes of *F. oxysporum* are expressed at different levels. However, the functionality of the truncated TORb protein remains unclear.

To ask whether TOR mediates nitrogen repression of invasive growth, we added rapamycin, a highly specific inhibitor of TOR. Rapamycin treatment restored cellophane penetration of *F. oxysporum* in the presence of repressing concentrations of ammonium (Figure 2B). Among different stress-inducing compounds tested, only rapamycin and, to a lesser extent, caffeine, which has also been reported as an inhibitor of TOR (Reinke et al., 2006), restored cellophane penetration on ammonium (Supplemental Figure 3 online). This indicates that the derepressing effect of rapamycin is associated with TOR inactivation and not a consequence of a general stress response.

Starvation of *S. cerevisiae* for single amino acids triggers a regulatory pathway known as the general amino acid control system, which results in activation of invasive growth at ammonium concentrations that normally inhibit this response (Braus et al., 2003). We tested whether starvation for a single amino acid could also restore cellophane penetration of *F. oxysporum* in the presence of ammonium by adding 3-amino-triazole (3AT), a histidine analog that induces histidine starvation (Hilton et al., 1965). In contrast to rapamycin, 3AT did not override the repressing effect of ammonium (Supplemental Figure 4 online), suggesting that the general amino acid control system does not play a major role in cellophane penetration. Collectively, these results indicate that 1) glutamine is a primary signal for nitrogen repression of cellophane invasion in *F. oxysporum,* and 2) transmission of the repressing signal requires the conserved protein kinase TOR.

Nitrogen repression of invasive growth is controlled by the bZIP protein MeaB and the wide domain regulator AreA

The *A. nidulans meaB* gene was identified by mutations conferring resistance to toxic amino acid analogues and methylammonium, resulting in derepression of nitrogen-regulated genes (Arst and Cove, 1973; Polley and Caddick, 1996). MeaB encodes a protein with a bZIP DNA-binding motif that mediates nitrogen metabolite repression in *A. nidulans* (Wong et al., 2007; Wong et al., 2008) (Figure 3A). A Blastp search of the *F. oxysporum* genome database identified a single MeaB orthologue, *FOXG_02277* (Supplemental Figure 5 online). We took advantage of the availability of a *F. oxysporum* Δ*meaB* mutant from a previous insertional mutagenesis screen (Lopez-Berges et al., 2009), to investigate the role of this bZIP factor in nitrogen regulation of cellophane penetration. The Δ*meaB* strain showed reduced growth on secondary nitrogen sources such as nitrate or nitrite, as well as resistance to DL-*p*-fluorophenylalanine and increased sensitivity to the toxic nitrate analogue chlorate (Figure 3B). While these phenotypes are very similar to those reported for the *meaB* mutant of *A. nidulans* (Polley and Caddick, 1996; Wong et al., 2007), we noted that the Δ*meaB* strain grew very poorly on ammonium as the sole nitrogen source (Figure 3B, compare growth on ammonium nitrate with ammonium sulfate or ammonium tartrate). Introduction of the *meaB* gene from *F. oxysporum* (*FomeaB*) or from *A. nidulans* (*AnmeaB*) into the Δ*meaB* mutant (Supplemental Figure 6 online) restored wild type growth on all nitrogen sources tested. We conclude that the role of MeaB in nitrogen utilization is highly conserved between *F. oxysporum* and *A. nidulans*.

A primary function of MeaB in nitrogen catabolite repression of *A. nidulans* is to inhibit the global regulator AreA via transcriptional activation of its co-repressor NmrA (Wong et al., 2007). To explore the role of AreA in nitrogen repression of cellophane penetration by *F. oxysporum*, a Δ*areA* null mutant was generated by replacing the entire coding region of the *areA* gene (*FOXG_03165*) with the hygromycin resistance cassette (Supplemental Figure 7A online). PCR analysis of hygromycin resistant transformants with different combinations of gene-specific primers identified one Δ*areA* strain showing homologous integration-mediated gene replacement (Supplemental Figure 7B-D online). Phenotypic

analysis of nitrogen utilization in the Δ*areA* mutant showed that it could only utilize glutamine and, to a much lesser extent, ammonium as nitrogen sources, and that it was highly resistant to chlorate (Figure 3B). Again, these phenotypes are highly similar to those reported for *areA* mutants of *A. nidulans* (Wilson and Arst, 1998) and *N. crassa* (Fu and Marzluf, 1987), although the growth phenotype on ammonium was more severe than in *A. nidulans*. The wild type growth pattern was completely restored by complementation of the mutant with the wild type *areA* gene (Figure 3B) (Supplemental Figure 7E online).

In *S. cerevisiae* and *A. nidulans,* mutations in downstream components of the TOR pathway confer increased resistance to rapamycin (Beck and Hall, 1999; Jacinto et al., 2001; Crespo and Hall, 2002; Fitzgibbon et al., 2005). We found that the Δ*meaB* and Δ*areA* mutants, but not the complemented strains, were silghtly more resistant to rapamycin than the wild type (Figure 3B). This suggests that MeaB and AreA may function downstream of TOR.

The Δ*meaB* strain was able to cross cellophane membranes even in the presence of repressing concentrations of ammonium, in contrast to the wild type or the strains complemented with either *FomeaB* or *AnmeaB* (Figure 4A). Thus, MeaB is required for ammonium-mediated repression of cellophane invasion in *F. oxysporum*. Interestingly, addition of rapamycin consistently enhanced penetration of the Δ*meaB* mutant on ammonium (Figure 4B), suggesting that MeaB and TOR have independent and additive roles in nitrogen repression of invasive growth.

We next tested the hypothesis that MeaB mediates nitrogen repression of cellophane penetration by inhibiting AreA. This would imply that AreA acts as a positive regulator of this virulence-associated process. Comparative cellophane penetration assays between the wild type strain and the Δ*areA* mutant were conducted on minimal medium supplemented with diluted (1:20) potato dextrose broth agar, due to the inability of the Δ*areA* strain to grow on nitrate as the sole nitrogen source. In contrast to our initial hypothesis, the Δ*areA* strain was still able to penetrate cellophane membranes. We conclude that AreA is not required for cellophane penetration in *F. oxysporum*. Unexpectedly, the Δ*areA* mutant retained some penetration ability on ammonium, albeit to a lesser extent than the Δ*meaB* strain. Cellophane penetration of the Δ*areA* strain on ammonium was further enhanced by rapamycin (Figure 4C). These results

suggest that the repressing role of MeaB on cellophane invasion is not mediated by inhibition of AreA. Rather, AreA itself seems to act as an ammonium-responsive repressor of cellophane penetration.

TOR and MeaB have partially independent roles in nitrogen catabolite repression

To further dissect the role of TOR, MeaB and AreA in nitrogen regulation of *F. oxysporum*, we measured transcript levels of three genes functioning in nitrogen catabolism: *nit1* encoding nitrate reductase (*FOXG_04181*), *nii1* encoding nitrite reductase (*FOXG_03192*), and *mepB* encoding an ammonium permease (*FOXG_08912*) (Teichert et al., 2008). Quantitative real time reverse transcription polymerase chain reaction (qRT-PCR) was performed on total RNA obtained from mycelia of the wild type, Δ*meaB,* Δ*areA* as well as the complemented strains, grown first on the derepressing source sodium nitrate and transferred for 3 h to sodium nitrate, ammonium nitrate or ammonium nitrate plus rapamycin. Transcript levels of *nit1, nii1* and *mepB* in the wild type strain were strongly decreased on ammonium, confirming that these genes are subject to nitrogen catabolite repression (Figure 5). Downregulation by ammonium was abolished in the Δ*meaB* mutant and restored in the complemented Δ*meaB*+*meaB* strain, indicating that this process requires MeaB. Induction of *nit1, nii1* and *mepB* by nitrate was not detected in the Δ*areA* mutant suggesting that it requires AreA.

Addition of rapamycin partially reversed ammonium repression of nitrogen catabolic genes in the wild type strain, directly implicating TOR in this process (Figure 5). Importantly, rapamycin treatment also increased transcript levels in the Δ*meaB* mutant. Thus, the role of TOR in nitrogen repression is at least partly independent of MeaB. By contrast, rapamycin failed to upregulate transcript levels of nitrogen catabolic genes in the Δ*areA* mutant. This suggests that TOR mediates nitrogen catabolite repression through inhibition of AreA.

We also measured transcript levels of the regulatory genes *nmr1*, *areA* and *meaB* in the different strains. Consistent with the postulated role of Nmr1 as a MeaB-dependent co-repressor of AreA (Wong et al., 2007; Wong et al., 2008),

nmr1 transcripts were upregulated on ammonium in the wild type strain but not in the Δ*meaB* mutant, indicating that MeaB is required for transcriptional upregulation of *nmr1* on ammonium (Figure 5). Transcript levels of *areA* on ammonium were inversely related to those of *nmr1*: downregulated in the wild type but unaffected in the Δ*meaB* strain. Rapamycin caused a significant increase in *areA* transcript levels on ammonium, both in the wild type and the Δ*meaB* mutant, further supporting the idea that TOR negatively regulates AreA through a MeaB-independent mechanism. Transcript levels of *meaB* were not influenced by nitrogen source. We noted that the complemented Δ*meaB*+*meaB* strain had higher *meaB* transcript levels than the wild type, possibly due to multiple copies of the complementing construct or to positional effects at the ectopic insertion site. Interestingly, *meaB* expression was upregulated in the Δ*areA* strain, and this increase was completely abolished by rapamycin. This result indicates that AreA and TOR function, respectively, as negative and positive regulators of *mea*B expression. Collectively, the data from the transcriptional analysis suggest that 1) TOR and MeaB have partially independent roles in nitrogen catabolite repression of *F. oxysporum*, and 2) both regulate transcript levels of *areA*.

Inactivation of TOR or MeaB does not bypass the requirement of the Fmk1 MAPK cascade for invasive growth

F. oxysporum mutants lacking the MAPK Fmk1 or its downstream component, the homeodomain transcription factor Ste12, fail to penetrate cellophane membranes even on permissive nitrogen sources such as sodium nitrate (Prados Rosales and Di Pietro, 2008; Rispail and Di Pietro, 2009). To explore the possible crosstalk between the activating MAPK cascade and the nitrogen repression pathway, a combination of pharmacological and genetic approaches was used. We first asked whether inactivation of TOR restored cellophane penetration in the Δ*fmk1* and Δ*ste12* mutants. However, neither of these mutants was able to cross cellophane membranes in the presence of rapamycin (Figure 7A). Second, we tested whether deletion of *meaB* could rescue cellophane penetration in a Δ*fmk1* background. A Δ*fmk1*Δ*meaB* double mutant

obtained by targeted gene knockout (see Materials and Methods for details) was still unable to penetrate cellophane membranes (Figure 6B). Thus, inactivation of either TOR or MeaB does not obviate the requirement of the MAPK Fmk1 for activation of invasive growth.

These results suggest that the nitrogen repression pathway controls cellophane penetration either independently or upstream of the Fmk1 MAPK cascade. To test whether MeaB and Fmk1 function in the same nitrogen regulation pathway, we compared the nitrogen utilization phenotypes of the Δ*fmk1* and Δ*meaB* single mutants with that of the Δ*fmk1*Δ*meaB* double mutant. All the strains showed similar growth as the wild type on rich nitrogen sources such as PDA or glutamine (Supplemental Figure 8 online). By contrast, the Δ*fmk1* and Δ*meaB* strains showed reduced growth on the non-preferred source, nitrate. Importantly, growth of the Δ*fmk1*Δ*meaB* double mutant on nitrate was even more reduced than in each single mutant, suggesting that loss of the two genes has an additive effect. This result supports the idea that MeaB and Fmk1 have separate roles in nitrogen regulation.

We next determined the effect of nitrogen source, *meaB* or *areA* deletion, and rapamycin on transcript levels of *ste12*. As previously reported for *C. lindemuthianum* (Hoi et al., 2007), the *ste12* gene of *F. oxysporum* produces two differentially spliced transcripts, one (*ste12*) containing the five predicted exons and the other (*ste12*Δ*E4*) lacking the fourth exon which encompasses part of the zinc finger (Rispail and Di Pietro, 2009). In the wild type strain grown on ammonium, levels of both *ste12* transcripts were approximately 75% lower than those on nitrate (Figure 6C). Ammonium-mediated repression of *ste12* was abolished in the Δ*meaB* and the Δ*areA* mutants and fully restored in the complemented strains. By contrast, rapamycin had no effect on *ste12* repression, suggesting that this process is not mediated by TOR. We conclude that ammonium downregulates expression of *ste12* in a MeaB- and AreA-dependent manner.

Ammonium negatively regulates vegetative hyphal fusion and root adhesion through TOR, MeaB and AreA

Besides cellophane penetration, the Fmk1 MAPK cascade controls additional virulence-related functions such as vegetative hyphal fusion, an ubiquitous process in filamentous fungi that mediates efficient adhesion of *F. oxysporum* to the roots of its host plant tomato (Prados Rosales and Di Pietro, 2008). To explore the role of nitrogen source in regulation of vegetative hyphal fusion, we determined the frequency of fusion events in *F. oxysporum* germlings grown on different nitrogen sources. The wild type strain showed a dramatic decrease of hyphal fusion events on ammonium nitrate compared to sodium nitrate (Figure 7A). The repressing effect of ammonium was completely reversed by addition of rapamycin. By contrast, fusion frequency of the Δ*meaB* strain on ammonium versus nitrate was increased rather than decreased. Fusion frequency of the Δ*areA* strain was as high as in the wild type, but was not reduced by ammonium. Thus, MeaB and AreA are required for repression of hyphal fusion by ammonium.

Vegetative hyphal fusion in liquid culture results in the formation of macroscopically visible mycelial aggregates (Prados Rosales and Di Pietro, 2008). When wild type microconidia were germinated on sodium nitrate, they formed dense hyphal networks that could not be disrupted by vigorous vortexing (Figure 7B). By contrast, these hyphal aggregates did not form on ammonium nitrate, most likely as a consequence of reduced hyphal fusion. Importantly, aggregate formation on ammonium was restored by rapamycin. The Δ*meaB* mutant produced hyphal aggregates independently of the nitrogen source. Complementation with the *meaB* gene from either *F. oxysporum* or *A. nidulans* restored ammonium repression (Supplemental Figure 9 online). The Δ*areA* mutant generally formed hyphal aggegates less efficiently than the wild type strain, probably due to its reduced growth. However, similar to the Δ*meaB* strain, aggregation of the Δ*areA* mutant was not repressed by ammonium (Figure 7B).

Root adhesion occurs during early stages of plant infection and contributes to virulence of *F. oxysporum* (Prados Rosales and Di Pietro, 2008). On sodium nitrate the wild type strain adhered efficiently to tomato roots, covering the root surface with a dense mycelium (Figure 7C). By contrast, on ammonium nitrate root adhesion was dramatically reduced, and this reduction was reversed by rapamycin treatment. Ammonium failed to repress root adhesion in the Δ*meaB*

and Δ*areA* strains. Taken together, these results suggest that distinct virulence-related functions are regulated by nitrogen status via the protein kinase TOR and the transcription factor MeaB. The global regulator AreA is not required for these functions and plays an active role in ammonium-mediated repression.

Nitrogen source and MeaB control infection of tomato plants

We next asked whether nitrogen source directly affected the ability of *F. oxysporum* to infect tomato plants. Roots of tomato seedlings were dip-inoculated with microconidia of the wild type, Δ*meaB* mutant or Δ*meaB+FomeaB* complemented strain. Seedlings were transferred to individual pots containing vermiculite and supplied either with 25 mM sodium nitrate or 25 mM ammonium nitrate. Disease symptoms in plants inoculated with the wild type strain and supplied with sodium nitrate increased steadily throughout the experiment, and most plants were dead 16 days after inoculation (Figure 8A). By contrast, plants supplied with ammonium nitrate showed a significant delay in symptom development and were still alive 23 days after inoculation. In plants infected with the Δ*meaB* strain, disease progression was slightly delayed, but in contrast to the wild type nitrogen source had no significant effect on the severity of disease syptoms. The complemented Δ*meaB+FomeaB* strain showed a similar virulence pattern as the wild type. We conclude that ammonium negatively regulates plant infection by *F. oxysporum* in a MeaB-dependent manner.

Disruption of the *areA* orthologue *fnr1* in *F. oxysporum* f. sp. *lycopersici* was previously shown to result in a delay of infection rate (Divon et al., 2006). We determined virulence of the Δ*areA* null mutant on tomato plants supplied either with sodium nitrate or ammonium nitrate. On sodium nitrate, the Δ*areA* strain showed a significant delay in the development of vascular wilt symptoms compared to the wild type (Supplemental Figure 10 online). However, in contrast to the wild type strain, disease severity of the Δ*areA* mutant was not further reduced in the presence of ammonium. These results confirm previous work showing that AreA contributes to virulence of *F. oxysporum* (Divon et al.,

2006). However, they also suggest that AreA contributes to ammonium-mediated repression of plant infection.

To explore the effect of nitrogen source on expression of virulence-related genes, we monitored transcript levels of the *six1* gene which is specifically induced *in planta* (van der Does et al., 2008), using real time qRT-PCR of total RNA obtained 48 hours after inoculation of microconidia on tomato roots supplied either with sodium nitrate or ammonium nitrate. At this early stage, *F. oxysporum* develops infection hyphae that penetrate the root surface and grow inter- and intracellularly within the root cortex (Figure 8B). Transcript levels of *six1* during infectious growth of the wild type strain were significantly reduced in the presence of ammonium compared to nitrate, but this decrease was not observed in the Δ*meaB* and Δ*areA* mutants (Figure 8C). Rapamycin treatment dramatically increased *six1* transcript levels in the three strains. This suggests that MeaB and TOR have independent functions in nitrogen regulation of the *in planta* expressed *six1* gene.

DISCUSSION

Fungi respond to the quantity and quality of nitrogen source by switching between distinct developmental programs, allowing them to maximize their potential for proliferation and survival (Schneper et al., 2004). In *S. cerevisiae*, nitrogen availability detemines the initiation of filamentous and invasive growth (Gimeno et al., 1992). Nitrogen status was also proposed to act as a regulatory switch for activating infectious development in plant pathogens (Snoeijers et al., 2000). Here we show that the preferred nitrogen source ammonium inhibits infection-related functions in the tomato vascular wilt pathogen *F. oxysporum*. Transmission of the nitrogen repression signal requires independent inputs from the conserved protein kinase TOR and the bZIP protein MeaB, two components that have not been associated previously with fungal pathogenicity on plants. A proposed model for nitrogen regulation of virulence-related functions in *F. oxysporum* is shown in Figure 9. Repression of invasive growth by ammonium was conserved in two other plant pathogens, *F. graminearum* and *M. oryzae,*

suggesting a general role for this nitrogen-response pathway in fungal pathogenicity on plants.

Control of virulence functions by nitrogen source

The preferred nitrogen source ammonium caused repression of cellophane invasion, vegetative hyphal fusion and root adhesion in *F. oxysporum*. We exploited the cellophane penetration assay to dissect the mechanism of nitrogen repression, using a combination of genetic and pharmacological approaches. This simple assay bears similarities with the invasive growth assay in yeast and displays a high level of correlation with the virulence phenotype of *F. oxysporum* on tomato plants. So far mutations in three distinct genes, encoding the MAPK Fmk1, the transcription factor Ste12 and the chitin synthase ChsV, were found to impair cellophane penetration in *F. oxysporum.* Strikingly, these mutations also abolish or severely reduce virulence on tomato plants (Madrid et al., 2003; Prados Rosales and Di Pietro, 2008; Rispail and Di Pietro, 2009). Thus, the ability to cross cellophane membranes defines a major pathogenicity function in *F. oxysporum.*

Cellophane invasion was inhibited by different sources of ammonium, including ammonium sulphate, ammonium tartrate and ammonium nitrate, but not by sodium nitrate. This suggests a repressing effect of the preferred nitrogen source ammonium rather than an activating effect of the poor source nitrate. Among additional nitrogen sources tested, only glutamine was able to partially repress invasive growth. Both ammonium and glutamine are readily assimilated by the cell and activate nitrogen catabolite repression in fungi (Marzluf, 1997; Caddick, 2004; Wong et al., 2008). In *S. cerevisiae* and *A. nidulans,* glutamine rather than ammonium was proposed to function as the major signal for nitrogen catabolite repression (Margelis et al., 2001; Crespo et al., 2002). We noted that the glutamine synthetase inhibitor MSX abolished the repressing effect of ammonium on cellophane penetration supporting the idea that glutamine is the main nitrogen signal for repression of virulence functions in *F. oxysporum* (Figure 9). However, a glutamine-independent effect of ammonium in nitrogen signalling cannot be ruled out. In *S. cerevisiae* ammonium was

shown to signal directly through the high affinity ammonium permease and sensor Mep2 to control filamentous growth and agar invasion (Lorenz and Heitman, 1998).

Role of TOR and MeaB in nitrogen repression

Rapamycin reversed the repressing effect of ammonium on virulence functions, implicating TOR as a negative regulator of at least three infection-related processes, invasive growth, cell fusion and cell-host adhesion. To our knowledge this is the first evidence for a direct role of TOR in the control of virulence mechanisms in a fungal plant pathogen. Recently, rapamycin was found to induce expression of adhesin genes and cellular aggregation in the human pathogen *Candida albicans* (Bastidas et al., 2009). Collectively this suggests a broadly conserved role of TOR in the control of infection-related processes in human and plant pathogens.

Besides TOR, genetic evidence also implicates the conserved bZIP protein MeaB in ammonium-mediated repression of virulence functions. In contrast to the wild type strain, the Δ*meaB* mutant displayed nitrogen source-independent activation of invasive growth, hyphal fusion and root adhesion. Moreover, MeaB was required for ammonium-mediated reduction of vascular wilt disease symptoms on tomato plants. These findings highlight a novel role of MeaB as a repressor of infection-related processes in *F. oxysporum* (Figure 9).

Both TOR and MeaB were associated previously with nitrogen regulation in fungi. While TOR is a key player in nitrogen catabolite repression of *S. cerevisiae* (Beck and Hall, 1999; Crespo and Hall, 2002), its role in filamentous fungi remains controversial. TOR was suggested to have only a minor function in nitrogen metabolism of *A. nidulans,* since mutations in TOR pathway genes did not have significant effects on the nitrogen utilization phenotype (Fitzgibbon et al., 2005). The discrepancy could partly be explained by the fact that several components of the TOR and nitrogen regulatory pathways such as Ure2, MeaB or Nmr1 are not conserved between *S. cerevisiae* and filamentous fungi. Here we showed that rapamycin treatment increases transcript levels of genes involved in nitrogen catabolism such as *nit1,* supporting a role of TOR in

nitrogen catabolite repression of *F. oxysporum*. This result is in agreement with a previous study showing that rapamycin activates expression of nitrogen metabolism-related genes such as ammonium permease and uricase in *F. fujikuroi* (Teichert et al., 2006).

How do MeaB and TOR control ammonium-mediated repression of nitrogen catabolism and virulence functions? We noted that MeaB is required for ammonium-induced upregulation of *nmr1* in *F. oxysporum,* as previously reported in *A. nidulans* (Wong et al., 2007). Moreover, the defects in nitrogen utilization of *F. oxysporum* and *A. nidulans* Δ*meaB* mutants were very similar, and the Δ*meaB* phenotype in *F. oxysporum* was successfully complemented by the *AnmeaB* gene. In both species, derepression of nitrogen catabolite genes in Δ*meaB* was strictly dependent on AreA. Collectively, these shared features suggest a similar mode of action of MeaB in nitrogen catabolite repression of *F. oxysporum* to that proposed in *A. nidulans* (Wong et al., 2007; Wong et al., 2008), whereby MeaB mediates transcriptional activation of the co-repressor Nmr1 which inhibits the wide domain regulator AreA (Figure 9).

A central question concerning the role of MeaB in nitrogen repression is how its activity is controlled by the nitrogen signal. An unexpected phenotype of the *F. oxysporum* Δ*meaB* mutant was its poor growth on ammonium as the sole nitrogen source (e.g. ammonium sulfate or ammonium tartrate). This phenotype was relieved in the presence of an additional nitrogen source (ammonium nitrate) and fully complemented by the *AnmeaB* gene, suggesting that MeaB has a conserved and previously uncharacterized role in ammonium utilization. The inability to use ammonium as a nitrogen source provides a straightforward explanation for the lack of ammonium-mediated repression in the Δ*meaB* strain. Further work is needed to elucidate the exact function of MeaB in ammonium utilization.

Our results, as well as those from *A. nidulans* (Wong et al., 2007), show that *meaB* transcript levels are unaffected by nitrogen source. In *F. fujikuroi* two *meaB* transcript sizes were detected, one of which was induced by nitrogen starvation (Schonig et al., 2008). While these results suggest that MeaB activity is regulated predominantly at the post-transcriptional or the post-translational level, we found that *meaB* transcript levels were upregulated in the Δ*areA*

mutant in a TOR-dependent manner. Thus, AreA and TOR may function, respectively, as negative and positive regulators of *mea*B expression.

In our study, *meaB* deletion or rapamycin treatment completely abolished ammonium-induced upregulation of *nmr1*. The lack of an additive effect of rapamycin in the Δ*meaB* mutant suggests that the ability of MeaB to activate *nmr1* may be controlled either directly or indirectly by TOR (Figure 9). Inspection of the amino acid sequences of fungal MeaB proteins revealed the presence of several highly conserved serine and threonine residues followed by a proline, which resemble the rapamycin-sensitive phosphorylation sites in the TOR-regulated yeast protein kinases Sch9 (Urban et al., 2007) and Npr1 (Gander et al., 2008). Moreover, deletion of MeaB resulted in a weak increase in rapamycin resistance. Further studies are needed to address the hypothesis that TOR controls MeaB activity in response to nitrogen source.

Besides the possible link between TOR and MeaB, two lines of evidence suggest that TOR also has MeaB-independent roles in nitrogen regulation. First, rapamycin-induced expression of nitrogen catabolic genes was detected both in the wild type and in the Δ*meaB* mutant. Second, cellophane penetration of the Δ*meaB* strain in the presence of ammonium was further increased by rapamycin treatment. These results support a model in which TOR has both MeaB-dependent and independent roles in ammonium-mediated repression of nitrogen catabolism and virulence functions (Figure 9).

Dual role for AreA as activator of nitrogen catabolic genes and repressor of virulence functions

The orthologous GATA factors Gln3 and AreA are strictly required for transcriptional activation of nitrogen catabolic genes in *S. cerevisiae* and *A. nidulans*, respectively (Crespo and Hall, 2002; Wong et al., 2008). Deletion of *areA* abolished nitrate-induced upregulation of *nit1, nii1* and *mepB*, suggesting that AreA functions as an activator of nitrogen catabolic genes in *F. oxysporum*. Importantly, rapamycin-mediated upregulation of these genes was also abolished in the Δ*areA* mutant. Similarly, in *F. fujikuroi* rapamycin was shown to activate AreA-regulated genes in the wild type but not in the Δ*areA* background

(Teichert et al., 2006). Moreover, a *gln3 gat1* double mutant of *S. cerevisiae* was blocked in rapamycin-mediated induction of the nitrogen-regulated genes *MEP2* and *GLN1* and was weakly resistant against rapamycin (Beck and Hall, 1999). Interestingly, the *F. oxysporum* Δ*areA* strain also showed a slight but consistent increase in rapamycin resistance. Taken together, these results indicate that TOR may mediate nitrogen catabolite repression in *F. oxysporum* by inhibiting the activity of the transcriptional activator AreA.

We initially hypothesized that AreA would function as a MeaB-controlled activator of virulence-related functions in *F. oxysporum*. However, two lines of evidence strongly argue against this hypothesis. First, the Δ*areA* mutant, although severely affected in growth due to its inability to utilize nitrogen sources other than ammonium or glutamine, was still able to perform cellophane penetration, hyphal fusion and root adhesion. This rules out a major activating role of AreA in these processes, and suggests that MeaB-mediated repression of virulence functions is independent of AreA (Figure 9). Generation of deletion and overexpression alleles of the cognate co-repressor *nmr1* should provide a rigorous test for this model.

Second, ammonium-mediated repression of virulence functions was partially relieved in the Δ*areA* mutant. The latter result was unexpected and suggests that AreA acts as a repressor of nitrogen-regulated virulence functions, in contrast to its well-described role as an activator of nitrogen catabolite genes (Figure 9). Previous evidence for a negative role of AreA in gene expression comes from a transcriptomic analysis in *F. fujikuroi,* which identified subsets of genes that were either down- or upregulated in the Δ*areA* mutant. The group of genes repressed by AreA included the glyoxylate cycle enzyme isocitrate lyase which links carbon to nitrogen metabolism, the autophagy-specific transcription factor IDI4 and the $NADP^+$-dependent glutamate dehydrogenase (Schonig et al., 2008). It remains to be determined whether the inhibitory role of AreA on virulence functions is mediated directly by transcriptional repression of target genes or indirectly through transcriptional activation of downstream repressors.

Nitrogen response pathway and Fmk1 MAPK cascade have opposing roles in the regulation of virulence

This study was initiated with the aim of exploring possible crosstalk between nitrogen signalling and the Fmk1 MAPK cascade in the control of virulence functions of *F. oxysporum*. Fmk1 is strictly required for invasive growth and pathogenicity on tomato plants, as well as for vegetative hyphal fusion and root adhesion (Di Pietro et al., 2001; Prados Rosales and Di Pietro, 2008). Here we show that these infection-related processes are negatively controlled by the preferred nitrogen source ammonium. We previously noted that cellophane penetration by *F. oxysporum* displays certain analogies to agar invasion in *S. cerevisiae*, since both processes require the orthologous MAPKs Fmk1 and Kss1, respectively, as well as the homeodomain transcription factor Ste12 (Madhani et al., 1997; Rispail and Di Pietro, 2009). This study reveals another common feature, repression by ammonium (Gimeno et al., 1992). In addition to invasive growth, two other virulence-related functions of *F. oxysporum*, hyphal fusion and root adhesion were also repressed by ammonium.

Both MeaB and TOR were required for ammonium-mediated repression of invasive growth. The inhibitory role of TOR detected in this work contrasts with a previous report which suggested a positive effect of TOR on pseudohyphal growth and agar invasion in yeast (Cutler et al., 2001). However, several lines of evidence favour a role for TOR as a repressor. First, invasive growth is generally stimulated by nitrogen limitation (Gimeno et al., 1992), a condition that inhibits TOR activity (Crespo and Hall, 2002; Crespo et al., 2002). Second, TOR inhibition by rapamycin activates expression of Mep2, an ammonium permease required for invasive growth (Lorenz and Heitman, 1998; Hardwick et al., 1999). Third, rapamycin treatment increased expression of hyphae-specific genes and promoted cell-cell adhesion in *C. albicans* (Bastidas et al., 2009). We therefore propose that the nitrogen-responsive TOR pathway and the filamentation/pathogenicity MAPK cascade, while acting on the same targets, have opposing roles in regulation of virulence-related functions.

A central question is how this shared yet opposing control is exerted. Pharmacological and genetic evidence indicate that the two pathways function independently, since neither rapamycin treatment nor deletion of *meaB* restored invasive growth in the Δ*fmk1* mutant. Moreover, the Δ*fmk1*Δ*meaB* double mutant displayed a more severe nitrogen regulation phenotype than the single

mutants. Previous studies highlighted the pivotal role of the homeodomain transcription factor Ste12 in regulating invasive growth and plant pathogenicity downstream of the MAPK cascade (Park et al., 2004; Rispail and Di Pietro, 2009). Interestingly, *ste12* transcript levels were strongly downregulated on ammonium compared to nitrate, suggesting that *ste12* expression is controlled by nitrogen source (Figure 9). Transcriptional repression of *ste12* in *F. oxysporum* required both MeaB and AreA, consistent with the phenotypic effects of Δ*meaB* and Δ*areA* mutations of reversing nitrogen repression of virulence functions, and further supporting the idea that AreA acts as a repressor of virulence-related genes such as *ste12*. Ammonium-mediated downregulation of *ste12* was not reversed by rapamycin, reinforcing the idea that, at least in part, MeaB and TOR function independently. However, it is still possible that TOR controls activity of Ste12 at the post-transcriptional level. We are currently addressing this hypothesis.

A second key issue concerns the common downstream targets regulated by the nitrogen response and MAPK pathways, and their role during invasive growth, adhesion and plant infection. Some of these genes are likely to encode extracellular or surface proteins. *six1*, for example, encodes a small secreted protein that is specifically induced during infection of tomato plants and contributes to virulence of *F. oxysporum* (Rep et al., 2004; van der Does et al., 2008). Expression of *six1* was dramatically repressed by ammonium in a manner dependent on MeaB and TOR. Full expression of the surface hydrophobin gene *MPG1* which is essential for pathogenicity of *M. oryzae*, also required nitrogen limitation and the Pmk1 MAPK (Lau and Hamer, 1996; Soanes et al., 2002). Other cellular responses associated with nitrogen starvation such as autophagy or generation of reactive oxygen species have recently been linked to fungal virulence on plants (Veneault-Fourrey et al., 2006; Egan et al., 2007; Brown et al., 2008). The possible role of the pathogenicity MAPK cascade in regulation of these processes has not been studied. More work is required to extend our understanding of how nitrogen and MAPK signalling interact to control infectious growth in plant pathogenic fungi.

METHODS

Fungal isolates and culture conditions

F. oxysporum f. sp. *lycopersici* race 2 wild type isolate 4287 (FGSC 9935) was used in all experiments. Generation and molecular characterization of the *F. oxysporum* Δ*fmk1*, Δ*ste12* and Δ*meaB* mutants was described previously (Di Pietro et al., 2001; Lopez-Berges et al., 2009; Rispail and Di Pietro, 2009). *F. graminearum* isolate PH-1 and *M. oryzae* isolate Guy-11 were used as indicated. All fungal strains were stored as microconidial suspensions at -80ºC with 30% glycerol. For extraction of genomic DNA and microconidia production, cultures were grown in potato dextrose broth (PDB; Difco, Detroit, MI) at 28ºC with shaking at 170 rpm (Di Pietro and Roncero, 1998). For analysis of gene expression, freshly obtained microconidia were germinated 14 h in PDB diluted 1:25 with water, supplemented with 25 mM $NaNO_3$. Mycelia were harvested by filtration, washed 3 times in sterile water and transferred for 3 h to liquid Minimal Medium (MM) (Puhalla, 1985) containing either 25 mM $NaNO_3$, or 25 mM NH_4NO_3 as the sole nitrogen source. Cellophane invasion assays were carried out as described (Prados Rosales and Di Pietro, 2008), using solid MM supplemented with 50 mM of the indicated nitrogen source. Amino acids were added after autoclaving. Rapamycin, L-methionine sulfoximine, caffeine, 3-amino-triazole, menadione and calcofluor white (all from Sigma) were added after autoclaving to the desired final concentrations from stock solutions prepared following suppliers instructions. For macro- and microscopic analysis of hyphal fusion and agglutination, fungal strains were grown 18 h in PDB diluted 1:25 with water and supplemented with 25 mM of the indicated nitrogen source, and observed in a Leica DMR microscope using the Nomarsky technique or a Leica binocular microscope. Photographs were recorded with a Leica DC 300F digital camera. For determination of colony growth, $2x10^4$ microconidia were spotted onto potato dextrose agar (PDA; Difco) with or without 2% (w/v) potassium chlorate, 250 µg ml^{-1} DL-*p*-fluorophenylalanine (PFA) or 150-200 ng ml^{-1} rapamycin, or MM agar containing either sodium glutamate, glutamine, $NaNO_3$, NH_4NO_3, $(NH_4)_2C_4H_4O_6$, $(NH_4)_2SO_4$ or $NaNO_2$ (all 25 mM) as nitrogen source. Plates were incubated at 28ºC for the indicated

time periods. All experiments included 2 replicate plates and were performed at least 3 times with similar results.

Nucleic acid manipulations

Total RNA and genomic DNA was extracted from *F. oxysporum* mycelium following previously reported protocols (Raeder and Broda, 1985; Chomczynski and Sacchi, 1987). Quality and quantity of extracted nucleic acids were determined by running aliquots in ethidium bromide stained agarose gels and by spectrophotometric analysis in a NanoDrop ND-1000 spectrophotometer (NanoDrop Technologies, USA), respectively. Routine nucleic acid manipulations were performed as described in standard protocols (Sambrook and Russell, 2001). DNA and protein sequence databases were searched using the BLAST algorithm (Altschul et al., 1990).

Quantitative real time reverse transcription PCR analysis

Total RNA was treated with deoxyribonuclease I (DNase I, Fermentas, USA) and reverse transcribed into first strand cDNA with ribonuclease inhibitor RNasin Plus RNase inhibitor (Promega, USA) and M-MLV reverse transcriptase (Invitrogen S.A., Spain) using a poly-dT antisense primer. Gene-specific primers (Supplemental Table 1 online) were designed to flank an intron if possible. RT-qPCR products were obtained using iQ SYBR Green Supermix (BioRad) and a iCycler iQ Real-time PCR System (BioRad). Transcript levels were calculated by comparative ΔCt and normalized to *act1*. Expression values are presented as values relative to the expression in the wild type strain under non-repressing conditions ($NaNO_3$).

Targeted gene knockout

Targeted replacement of the *F. oxysporum meaB* gene in the Δ*fmk1* background was performed using a fusion PCR construct and protocol described previously (Lopez-Berges et al., 2009). Targeted replacement of the entire coding region of the *F. oxysporum areA* gene was performed using the split-marker method (Catlett et al., 2003), following the protocol previously described (Rispail and Di Pietro, 2009). PCR reactions were routinely performed with the High Fidelity Template PCR system (Roche Diagnostics SL) using a MJ Mini BioRad personal thermal cycler. DNA fragments flanking the *areA* coding region were amplified from genomic DNA of *F. oxysporum* with primer pairs areA-1 + areA-M13-1 and areA-2 + areA-M13-2 respectively (Supplemental Table 1 online; Supplemental Figure 5 online) and PCR-fused with partially overlapping truncated versions of the hygromycin B resistance cassette, using primer combinations areA-1n + Hyg-G and areA-2n + Hyg-Y respectively. The obtained split-marker fragments were used to cotransform protoplasts of the *F. oxysporum* wild type strain to hygromycin resistance, and transformants were purified by monoconidial isolation as described (Di Pietro and Roncero, 1998). Transformants showing homologous insertion of the construct were detected by PCR of genomic DNA with primer pairs areA-3 + hyg-6, areA-1n + areA-2n and areA-4 + areA-5 (Supplemental Figure 5B, C and D online).

Complementation of *meaB* and *areA* deletion mutants

To generate a construct for complementing the *meaB* deletion mutants, a 4334 bp fragment, spanning from 1981 bp upstream of the wild type *F. oxysporum meaB* translation initiation codon to 832 bp downstream of the translation termination codon, was amplified by PCR using the High Fidelity Template PCR system (Roche Diagnostics SL) with primer pairs FomeaB-For + FomeaB-Rev. For complementing with the heterologous *Aspergillus nidulans meaB* gene, a 4486 bp fragment, spanning from 1934 bp upstream of the wild type *A. nidulans meaB* translation initiation codon to 911 bp downstream of the translation termination codon, was amplified with primer pairs AnmeaB-For + AnmeaB-Rev. Both amplified fragments were used to cotransform protoplasts of the

meaB deletion mutant with the phleomycin resistance cassette. 3 out of 25 phleomycin resistance cotransformants were selected in both complementation experiments for their wild type growth phenotype in the presence of the toxic nitrate analogue chlorate and analyzed for the presence of a functional *meaB* allele by PCR with gene-specific primer pairs 6G5-5 + 6G5-6 and AnmeaB-1 + AnmeaB-2, for homologous and heterologous complementation respectively. A 346 bp and a 287 bp amplification products were detected in the respectively selected phleomycin resistant cotransformants but not in the Δ*meaB* strain (Supplemental Figure 6 online). We concluded that these transformants, designated Δ*meaB + FomeaB* and Δ*meaB + AnmeaB*, had integrated an intact copy of the *F. oxysporum* and the *A. nidulans meaB* gene into the genome respectively.

For the complementation of the *areA* deletion mutant, a 6463 bp fragment, spanning from 1931 bp upstream of the wild type *areA* translation initiation codon to 1572 bp downstream of the translation termination codon, was amplified with primer pairs areA-3 + areA-2. The amplified fragment was used to cotransform protoplasts of the *areA* deletion mutant with the phleomycin resistance cassette. 3 out of 15 phleomycin resistance cotransformants were selected for their wild type growth phenotype in the presence of nitrate as the sole nitrogen source and analyzed for the presence of a functional *areA* allele by PCR with gene-specific primers areA-4 + areA-5. A 438 bp amplification product was detected in the selected phleomycin resistant cotransformants but not in the Δ*areA* strain (Supplemental Figure 7 online). We concluded that these transformants, designated Δ*areA + areA*, had integrated an intact copy of the *F. oxysporum areA* gene into the genome.

Virulence and root adhesion assays

Tomato plant inoculation assays were performed in a growth chamber as described (Di Pietro and Roncero, 1998). Plants were supplied either with 25 mM $NaNO_3$ or 25 mM NH_4NO_3 solutions in water. At different times after inoculation, severity of disease symptoms was recorded using an index ranging from 1 (healthy plant) to 5 (dead plant). Ten plants were used for each

treatment. Inoculations for expression analysis *in planta* and root adhesion assays were performed as described (Di Pietro et al., 2001). Virulence and root adhesion experiments were performed at least three times with similar results.

SUPPLEMENTAL DATA

Supplemental Figures

Supplemental Figure 1. Effect of carbon source on cellophane penetration by *Fusarium oxysporum*.

Supplemental Figure 2. Expression of *Fusarium oxysporum tor1a* and *tor1b* genes.

Supplemental Figure 3. Cellophane penetration on ammonium is specifically induced by TOR inhibition, but not by salt, oxidative or cell wall stress.

Supplemental Figure 4. Nitrogen regulation of invasive growth is not mediated by the general amino acid control system.

Supplemental Figure 5. Amino acid sequence alignment of fungal orthologues of the bZIP protein MeaB.

Supplemental Figure 6. Complementation of the *Fusarium oxysporum meaB* deletion mutant with *FomeaB* or *AnmeaB*.

Supplemental Figure 7. Targeted deletion of the *Fusarium oxysporum areA* gene.

Supplemental Figure 8. Nitrogen utilization phenotypes caused by single and double deletion of *meaB* and *fmk1*.

Supplemental Figure 9. Nitrogen source regulates hyphal aggregation via TOR and MeaB.

Supplemental Figure 10. AreA contributes to virulence of *Fusarium oxysporum* on tomato plants independently of nitrogen source.

Supplemental Tables

Supplemental Table 1. List of primers used in this study.

ACKNOWLEDGEMENTS

The authors are grateful to Esther Martínez Aguilera for valuable technical assistance. This research was supported by grant BIO2007-62661 from the Ministerio de Educación y Ciencia and by the Marie Curie Research Training Network MRTN-CT-2005-019277 (SIGNALPATH). M.S.L.B. and R.P.R. had PhD fellowships from the Ministerio de Educación y Ciencia.

FIGURE LEGENDS

Figure 1. Nitrogen source regulates cellophane penetration in plant pathogenic fungi.

A. Effect of nitrogen source on penetration of cellophane membranes by *Fusarium oxysporum*. Fungal colonies were grown 4 days at 28ºC on plates with minimal medium containing 50 mM of the indicated nitrogen source, covered with a cellophane membrane (before). The cellophane with the fungal colony was removed and plates were incubated for an additional day to determine the presence of mycelial growth on the plate (after). **B.** Cellophane penetration of *Fusarium graminearum* and *Magnaporthe oryzae* on the indicated nitrogen source was determined as in (**A**).

Figure 2. Ammonium repression of invasive growth is mediated by glutamine synthetase and the protein kinase TOR.

A. Model of TOR pathway activation by glutamine (adapted from Crespo *et al.* 2002). GS, glutamine synthetase; MSX, L-methionine sulfoximine. **B.** Cellophane penetration was determined on plates containing 50 mM $NaNO_3$, glutamine or NH_4NO_3 with or without 10 mM MSX, a specific inhibitor of glutamine synthetase, or 150 ng ml^{-1} rapamycin, a specific inhibitor of TOR.

Figure 3. Effect of *meaB* and *areA* deletion on nitrogen utilization of *Fusarium oxysporum*.

A. Model of regulation of nitrogen catabolic genes in *Aspergillus nidulans* by MeaB (adapted from Wong *et al.* 2008) **B.** Growth of the indicated strains on different nitrogen sources (see Methods). Cultures were grown 3 days at 28ºC, except on NH_4NO_3, $(NH_4)_2C_4H_4O_6$, $(NH_4)_2SO_4$ and PDA + rapamycin (5 days). PDA, potato dextrose agar; PFA, DL-*p*-fluorophenylalanine. Bar 5 mm.

Figure 4. Ammonium repression of invasive growth is controlled by the bZIP protein MeaB and the wide domain regulator AreA.

A. Deletion of *meaB* causes invasive growth in the presence of 50 mM of the repressing nitrogen source NH_4NO_3. The indicated strains were grown 4 days before removing the cellophane membrane. **B.** MeaB and TOR have additive functions in ammonium-mediated repression of invasive growth. Fungal colonies were grown 3 days before removing the cellophane membrane to quantitatively compare invasion rate. Bar 5 mm. **C.** AreA is not required for invasive growth and contributes to ammonium-mediated repression of this process. Cellophane penetration of the Δ*areA* mutant was determined after 4 days incubation on plates containing PDA, or PDB diluted 1:25 with water and supplemented with 50 mM NH_4NO_3 or NH_4NO_3 + 150 ng ml^{-1} rapamycin.

Figure 5. Effect of nitrogen source, *meaB* or *areA* deletion, and rapamycin on transcript levels of nitrogen catabolic and regulatory genes.

Quantitative real time RT-PCR analysis was performed in the indicated strains germinated 14 h in PDB diluted 1:25 with water supplemented with 25 mM $NaNO_3$, then washed with water and transferred for 3 h to 25 mM $NaNO_3$ (black columns), 25 mM NH_4NO_3 (dark grey columns) or 25 mM NH_4NO_3 + 150 ng ml^{-1} rapamycin (light grey columns) as the sole nitrogen source. Relative transcript levels represent mean ΔCt values of nitrogen catabolic genes *nit1* (nitrate reductase), *nii1* (nitrite reductase) and *mepB* (ammonium permease), as well as nitrogen regulatory genes *nmr1* (co-repressor), *areA* and *meaB*, normalized to the *act1* gene and expressed relative to transcript levels of the wild type strain on $NaNO_3$. Bars represent standard errors from 3 independent experiments with 3 replicates each.

Figure 6. Inactivation of TOR or MeaB does not bypass the requirement of the Fmk1 MAPK cascade for invasive growth.

A, B. Cellophane penetration in mutants lacking the MAPK Fmk1 or the transcription factor Ste12 is not restored by 150 ng ml^{-1} rapamycin (**A**) or by *meaB* deletion (**B**). **C.** Expression of *ste12* is repressed by nitrogen source via MeaB and AreA. Quantitative real time RT-PCR analysis was performed in the indicated strains germinated as described in Figure 5 and transferred for 3 h to $NaNO_3$ (black columns), NH_4NO_3 (dark grey columns) or NH_4NO_3 + 150 ng ml^{-1} rapamycin (light grey columns). Relative transcript levels represent mean ΔCt values of differentially spliced transcripts *ste12* (containing the five predicted exons) and *ste12ΔE4* (lacking exon 4), normalized to *act1* and expressed relative to transcript levels of *ste12* in the wild type strain on $NaNO_3$. Bars represent standard errors from 3 independent experiments with 3 replicates each.

Figure 7. Nitrogen source regulates vegetative hyphal fusion, hyphal aggregation and root adhesion via TOR and MeaB.

A. Frequency of vegetative hyphal fusion of the indicated strains after 18 h of conidial germination in PDB diluted 1:25 with water and supplemented with 25 mM of the indicated nitrogen source was determined microscopically and expressed as percentage of fused germlings versus total number of germlings. Bars represent standard errors from 3 independent experiments with 3 replicates each. **B.** Hyphal aggregates forming after 36 h conidial germination under conditions described in (**A**). Cultures were vortexed to dissociate weakly adhered hyphae and observed in a binocular microscope. **C.** Root adhesion assay. Roots of tomato seedlings were immersed for 36 h in microconidial suspensions of the indicated strains in PDB diluted 1:25 with water and supplemented with 25 mM of the indicated nitrogen source, then washed by vigorous shaking in water and observed in a binocular microscope. Adhering fungal mycelium is visible as a white mass covering the roots.

Figure 8. Nitrogen source and MeaB control infection of tomato plants.

A. Incidence of *Fusarium* wilt on tomato plants (cultivar Monica) inoculated with the wild type strain (black symbols), the Δ*meaB* mutant (grey symbols) and the

Δ*meaB + FomeaB* complemented strain (white symbols). Plants were supplied either with 25 mM $NaNO_3$ (squares) or 25 mM NH_4NO_3 (circles) solutions in water. Uninoculated plants supplied with 25 mM $NaNO_3$ (dark grey diamonds) were used as controls. Severity of disease symptoms was recorded at the indicated times using an index ranging from 1 (healthy plant) to 5 (dead plant). Bars represent standard errors calculated from 10 plants. **B.** Penetration of tomato roots by infection hyphae of *F. oxysporum.* Roots of tomato seedlings were immersed for 24 h in a microconidial suspension of the wild type strain in the presence of 25 mM $NaNO_3$ and observed microscopically. Arrows point to sites of penetration. Bar 10 µm. **C.** Quantitative real time RT-PCR analysis of the plant-induced virulence effector gene *six1* in different *F. oxysporum* strains 48 h after inoculation on tomato roots supplied with 25 mM $NaNO_3$ (black columns), 25 mM NH_4NO_3 (dark grey columns) or 25 mM NH_4NO_3 + 150 ng ml^{-1} rapamycin (light grey columns) as the sole nitrogen source. Relative transcript levels represent mean ΔCt values of *six1* normalized to *act1* and expressed relative to transcript levels of the wild type strain on $NaNO_3$. Bars represent standard errors from 3 independent experiments with 3 replicates each.

Figure 9. Nitrogen controls virulence functions in *Fusarium oxysporum* through TOR and MeaB.

The preferred nitrogen source ammonium represses virulence functions via glutamine synthetase, the protein kinase TOR, the bZIP protein MeaB and the GATA factor AreA. Thick lines indicate results based on genetic or pharmacological evidence, thin lines indicate results based on expression analysis. Ammonium depletion, MSX or rapamycin lead to inactivation of TOR and/or MeaB, thus promoting virulence functions. TOR mediates repression of nitrogen catabolic genes and virulence functions both by MeaB-dependent and independent mechanisms. AreA has a dual role as an activator of nitrogen catabolic genes and as a repressor of virulence functions. The MAPK Fmk1 and the downstream homeodomain transcription factor Ste12 are required for activation of virulence functions through a positive regulatory pathway. Ammonium represses *ste12* expression through MeaB and AreA. A possible

role of the nitrogen repression pathway upstream of Fmk1 cannot be excluded.

TABLES

Table 1. Effect of different nitrogen sources on cellophane penetration by *Fusarium oxysporum*. Fungal colonies were grown 4 days at 28ºC on plates with minimal medium containing the indicated nitrogen source, covered with a cellophane membrane. The cellophane with the fungal colony was removed, plates were incubated for an additional day and presence of fungal mycelium on the underlying medium was scored.

Nitrogen source [50 mM]	Cellophane penetration
$NaNO_3$	+
NH_4NO_3	-
$(NH_4)_2SO_4$	-
$(NH_4)_2C_4H_4O_6$	-
Casaminoacids	+
Arginine	+
Glutamate	+
Glutamine	+/-
Methionine	+
Proline	+

REFERENCES

Altschul, S.F., Gish, W., Miller, W., Myers, C.W., and Lipman, D.L. (1990). Basic local alignment search tool. J Mol Biol **215,** 403-410.

Arst, H.N., Jr., and Cove, D.J. (1973). Nitrogen metabolite repression in Aspergillus nidulans. Mol Gen Genet **126,** 111-141.

Bastidas, R.J., Heitman, J., and Cardenas, M.E. (2009). The protein kinase Tor1 regulates adhesin gene expression in *Candida albicans*. PLoS Pathog **5,** e1000294.

Beck, T., and Hall, M.N. (1999). The TOR signalling pathway controls nuclear localization of nutrient-regulated transcription factors. Nature **402,** 689-692.

Braus, G.H., Grundmann, O., Bruckner, S., and Mosch, H.U. (2003). Amino acid starvation and Gcn4p regulate adhesive growth and *FLO11* gene expression in *Saccharomyces cerevisiae*. Mol Biol Cell **14,** 4272-4284.

Brown, S.H., Yarden, O., Gollop, N., Chen, S., Zveibil, A., Belausov, E., and Freeman, S. (2008). Differential protein expression in *Colletotrichum acutatum*: changes associated with reactive oxygen species and nitrogen starvation implicated in pathogenicity on strawberry. Mol Plant Pathol **9,** 171-190.

Caddick, M.X. (2004). Nitrogen regulation in mycelial fungi. In Biochemistry and molecular biology. The Mycota III, 2nd ed., R. Brambl and G.A. Marzluf, eds (Berlin, Germany: Springer Verlag), pp. 349-368.

Caddick, M.X., Arst, H.N., Jr., Taylor, L.H., Johnson, R.I., and Brownlee, A.G. (1986). Cloning of the regulatory gene *areA* mediating nitrogen metabolite repression in *Aspergillus nidulans*. EMBO J **5,** 1087-1090.

Catlett, N.L., Lee, B.N., Yoder, O.C., and Turgeon, B.G. (2003). Split-Marker Recombination for Efficient Targeted Deletion of Fungal Genes. Fungal Genet Newsl **50,** 9-11.

Coleman, M., Henricot, B., Arnau, J., and Oliver, R.P. (1997). Starvation-induced genes of the tomato pathogen *Cladosporium fulvum* are also induced during growth *in planta*. Mol Plant Microbe Interact **10,** 1106-1109.

Crespo, J.L., and Hall, M.N. (2002). Elucidating TOR signaling and rapamycin action: lessons from *Saccharomyces cerevisiae*. Microbiol Mol Biol Rev **66,** 579-591.

Crespo, J.L., Powers, T., Fowler, B., and Hall, M.N. (2002). The TOR-controlled transcription activators GLN3, RTG1, and RTG3 are regulated in response to intracellular levels of glutamine. Proc Natl Acad Sci U S A **99,** 6784-6789.

Cutler, N.S., Pan, X., Heitman, J., and Cardenas, M.E. (2001). The TOR signal transduction cascade controls cellular differentiation in response to nutrients. Mol Biol Cell **12,** 4103-4113.

Chomczynski, P., and Sacchi, N. (1987). Single-step method of RNA isolation by acid guanidinium thiocyanate-phenol-chloroform extraction. Anal Biochem **162,** 156-159.

De Virgilio, C., and Loewith, R. (2006). Cell growth control: little eukaryotes make big contributions. Oncogene **25,** 6392-6415.

Dementhon, K., Paoletti, M., Pinan-Lucarre, B., Loubradou-Bourges, N., Sabourin, M., Saupe, S.J., and Clave, C. (2003). Rapamycin mimics the incompatibility reaction in the fungus *Podospora anserin*a. Eukaryot Cell **2,** 238-246.

Di Pietro, A., and Roncero, M.I. (1998). Cloning, expression, and role in pathogenicity of *pg1* encoding the major extracellular endopolygalacturonase of the vascular wilt pathogen *Fusarium oxysporum*. Mol Plant Microbe Interact **11,** 91-98.

Di Pietro, A., Garcia-Maceira, F.I., Meglecz, E., and Roncero, M.I. (2001). A MAP kinase of the vascular wilt fungus *Fusarium oxysporum* is essential for root penetration and pathogenesis. Mol Microbiol **39,** 1140-1152.

Divon, H., Rothan-Denoyes, B., Davydov, O., Di Pietro, A., and Fluhr, R. (2005). Nitrogen-responsive genes are differentially regulated in planta during *Fusarium oxysporum* f. sp. *lycopersici* infection. Mol Plant Pathol **6,** 459-470.

Divon, H., Ziv, C., Davydov, O., Yarden, O., and Fluhr, R. (2006). The global nitrogen regulator, FNR1, regulates fungal nutrition-genes and fitness during *Fusarium oxysporum* pathogenesis. Mol. Plant Pathol. **7,** 485-497.

Donofrio, N.M., Oh, Y., Lundy, R., Pan, H., Brown, D.E., Jeong, J.S., Coughlan, S., Mitchell, T.K., and Dean, R.A. (2006). Global gene expression during nitrogen starvation in the rice blast fungus, *Magnaporthe grisea*. Fungal Genet Biol **43,** 605-617.

Egan, M.J., Wang, Z.Y., Jones, M.A., Smirnoff, N., and Talbot, N.J. (2007). Generation of reactive oxygen species by fungal NADPH oxidases is required for rice blast disease. Proc Natl Acad Sci U S A **104,** 11772-11777.

Fitzgibbon, G.J., Morozov, I.Y., Jones, M.G., and Caddick, M.X. (2005). Genetic analysis of the TOR pathway in *Aspergillus nidulans*. Eukaryot Cell **4,** 1595-1598.

Froeliger, E.H., and Carpenter, B.E. (1996). *NUT1*, a major nitrogen regulatory gene in *Magnaporthe grisea*, is dispensable for pathogenicity. Mol Gen Genet **251,** 647-656.

Fu, Y.H., and Marzluf, G.A. (1987). Characterization of *nit-2*, the major nitrogen regulatory gene of *Neurospora crassa*. Mol Cell Biol **7,** 1691-1696.

Fu, Y.H., and Marzluf, G.A. (1990). *nit-2*, the major positive-acting nitrogen regulatory gene of *Neurospora crassa*, encodes a sequence-specific DNA-binding protein. Proc Natl Acad Sci U S A **87,** 5331-5335.

Gander, S., Bonenfant, D., Altermatt, P., Martin, D.E., Hauri, S., Moes, S., Hall, M.N., and Jenoe, P. (2008). Identification of the rapamycin-sensitive phosphorylation sites within the Ser/Thr-rich domain of the yeast Npr1 protein kinase. Rapid Commun Mass Spectrom **22,** 3743-3753.

Gimeno, C.J., Ljungdahl, P.O., Styles, C.A., and Fink, G.R. (1992). Unipolar cell divisions in the yeast *S. cerevisiae* lead to filamentous growth: regulation by starvation and RAS. Cell **68,** 1077-1090.

Hardwick, J.S., Kuruvilla, F.G., Tong, J.K., Shamji, A.F., and Schreiber, S.L. (1999). Rapamycin-modulated transcription defines the subset of nutrient-sensitive signaling pathways directly controlled by the Tor proteins. Proc Natl Acad Sci U S A **96,** 14866-14870.

Hilton, J.L., Kearney, P.C., and Ames, B.N. (1965). Mode of action of the herbicide, 3-amino-1,2,4-triazole(amitrole): inhibition of an enzyme of histidine biosynthesis. Arch Biochem Biophys **112,** 544-547.

Hoi, J.W., Herbert, C., Bacha, N., O'Connell, R., Lafitte, C., Borderies, G., Rossignol, M., Rouge, P., and Dumas, B. (2007). Regulation and role of a STE12-like transcription factor from the plant pathogen *Colletotrichum lindemuthianum*. Mol Microbiol **64,** 68-82.

Jacinto, E., Guo, B., Arndt, K.T., Schmelzle, T., and Hall, M.N. (2001). TIP41 interacts with TAP42 and negatively regulates the TOR signaling pathway. Mol Cell **8,** 1017-1026.

Jansen, C., von Wettstein, D., Schafer, W., Kogel, K.H., Felk, A., and Maier, F.J. (2005). Infection patterns in barley and wheat spikes inoculated with wild-type and trichodiene synthase gene disrupted *Fusarium graminearum*. Proc Natl Acad Sci U S A **102,** 16892-16897.

Lau, G., and Hamer, J.E. (1996). Regulatory Genes Controlling *MPG1* Expression and Pathogenicity in the Rice Blast Fungus *Magnaporthe grisea*. Plant Cell **8,** 771-781.

Lopez-Berges, M.S., A, D.I.P., Daboussi, M.J., Wahab, H.A., Vasnier, C., Roncero, M.I., Dufresne, M., and Hera, C. (2009). Identification of virulence genes in *Fusarium oxysporum* f. sp. *lycopersici* by large-scale transposon tagging. Mol Plant Pathol **10,** 95-107.

Lorenz, M.C., and Heitman, J. (1998). The MEP2 ammonium permease regulates pseudohyphal differentiation in *Saccharomyces cerevisiae*. EMBO J **17,** 1236-1247.

Madhani, H.D., and Fink, G.R. (1997). Combinatorial control required for the specificity of yeast MAPK signaling. Science **275,** 1314-1317.

Madhani, H.D., Styles, C.A., and Fink, G.R. (1997). MAP kinases with distinct inhibitory functions impart signaling specificity during yeast differentiation. Cell **91,** 673-684.

Madrid, M.P., Di Pietro, A., and Roncero, M.I. (2003). Class V chitin synthase determines pathogenesis in the vascular wilt fungus *Fusarium oxysporum* and mediates resistance to plant defence compounds. Mol Microbiol **47,** 257-266.

Margelis, S., D'Souza, C., Small, A.J., Hynes, M.J., Adams, T.H., and Davis, M.A. (2001). Role of glutamine synthetase in nitrogen metabolite repression in *Aspergillus nidulans*. J Bacteriol **183,** 5826-5833.

Marzluf, G.A. (1997). Genetic regulation of nitrogen metabolism in the fungi. Microbiol Mol Biol Rev **61,** 17-32.

Park, G., Bruno, K.S., Staiger, C.J., Talbot, N.J., and Xu, J.R. (2004). Independent genetic mechanisms mediate turgor generation and penetration peg formation during plant infection in the rice blast fungus. Mol Microbiol **53,** 1695-1707.

Pellier, A.L., Lauge, R., Veneault-Fourrey, C., and Langin, T. (2003). CLNR1, the AREA/NIT2-like global nitrogen regulator of the plant fungal pathogen *Colletotrichum lindemuthianum* is required for the infection cycle. Mol Microbiol **48,** 639-655.

Perez-Garcia, A., Snoeijers, S.S., Joosten, M.H., Goosen, T., and De Wit, P.J. (2001). Expression of the Avirulence gene *Avr9* of the fungal tomato pathogen *Cladosporium fulvum* is regulated by the global nitrogen response factor NRF1. Mol Plant Microbe Interact **14,** 316-325.

Polley, S.D., and Caddick, M.X. (1996). Molecular characterisation of *meaB*, a novel gene affecting nitrogen metabolite repression in *Aspergillus nidulans*. FEBS Lett **388,** 200-205.

Poulter, R.T., Goodwin, T.J., and Butler, M.I. (2003). Vertebrate helentrons and other novel Helitrons. Gene **313,** 201-212.

Prados Rosales, R.C., and Di Pietro, A. (2008). Vegetative hyphal fusion is not essential for plant infection by *Fusarium oxysporum*. Eukaryot Cell **7,** 162-171.

Puhalla, J.E. (1985). Classification of strains of *Fusarium oxysporum* on the basis of vegetative incompatibility. Can. J. Bot. **63,** 179-183.

Raeder, U., and Broda, P. (1985). Rapid preparation of DNA from filamentous fungi. Lett Appl Microbiol **1,** 17-20.

Reinke, A., Chen, J.C., Aronova, S., and Powers, T. (2006). Caffeine targets TOR complex I and provides evidence for a regulatory link between the FRB and kinase domains of Tor1p. J Biol Chem **281,** 31616-31626.

Rep, M., van der Does, H.C., Meijer, M., van Wijk, R., Houterman, P.M., Dekker, H.L., de Koster, C.G., and Cornelissen, B.J. (2004). A small, cysteine-rich protein secreted by *Fusarium oxysporum* during colonization of xylem vessels is required for *I-3*-mediated resistance in tomato. Mol Microbiol **53,** 1373-1383.

Rispail, N., and Di Pietro, A. (2009). *Fusarium oxysporum* Ste12 controls invasive growth and virulence downstream of the Fmk1 MAPK cascade. Mol Plant Microbe Interact **22,** 830-839.

Rohde, J.R., Bastidas, R., Puria, R., and Cardenas, M.E. (2008). Nutritional control via Tor signaling in *Saccharomyces cerevisiae*. Curr Opin Microbiol **11,** 153-160.

Sambrook, J., and Russell, D.W. (2001). Molecular cloning: A laboratory manual. (New York: Cold Spring Harbor Laboratory Press).

Schneper, L., Duvel, K., and Broach, J.R. (2004). Sense and sensibility: nutritional response and signal integration in yeast. Curr Opin Microbiol **7,** 624-630.

Schonig, B., Brown, D.W., Oeser, B., and Tudzynski, B. (2008). Cross-species hybridization with *Fusarium verticillioides* microarrays reveals new insights into *Fusarium fujikuroi* nitrogen regulation and the role of AreA and NMR. Eukaryot Cell **7,** 1831-1846.

Snoeijers, S.S., Perez-Garcia, A., Joosten, M.H., and De Wit, P.J. (2000). The effect of nitrogen on disease development and gene expression in bacterial and fungal plant pathogens. Eur. J. Plant Pathol. **106,** 493-506.

Soanes, D.M., Kershaw, M.J., Cooley, R.N., and Talbot, N.J. (2002). Regulation of the *MPG1* hydrophobin gene in the rice blast fungus *Magnaporthe grisea*. Mol Plant Microbe Interact **15,** 1253-1267.

Stephenson, S.A., Green, J.R., Manners, J.M., and Maclean, D.J. (1997). Cloning and characterisation of glutamine synthetase from *Colletotrichum gloeosporioides* and demonstration of elevated expression during pathogenesis on *Stylosanthes guianensis*. Curr Genet **31,** 447-454.

Talbot, N.J. (2003). On the trail of a cereal killer: Exploring the biology of *Magnaporthe grisea*. Annu Rev Microbiol **57,** 177-202.

Talbot, N.J., Ebbole, D.J., and Hamer, J.E. (1993). Identification and characterization of *MPG1*, a gene involved in pathogenicity from the rice blast fungus *Magnaporthe grisea*. Plant Cell **5,** 1575-1590.

Teichert, S., Wottawa, M., Schonig, B., and Tudzynski, B. (2006). Role of the *Fusarium fujikuroi* TOR kinase in nitrogen regulation and secondary metabolism. Eukaryot Cell **5,** 1807-1819.

Teichert, S., Rutherford, J.C., Wottawa, M., Heitman, J., and Tudzynski, B. (2008). Impact of ammonium permeases mepA, mepB, and mepC on nitrogen-regulated secondary metabolism in *Fusarium fujikuroi*. Eukaryot Cell **7,** 187-201.

Urban, J., Soulard, A., Huber, A., Lippman, S., Mukhopadhyay, D., Deloche, O., Wanke, V., Anrather, D., Ammerer, G., Riezman, H., Broach, J.R., De Virgilio, C., Hall, M.N., and Loewith, R. (2007). Sch9 is a major target of TORC1 in *Saccharomyces cerevisiae*. Mol Cell **26,** 663-674.

Van den Ackerveken, G.F., Dunn, R.M., Cozijnsen, A.J., Vossen, J.P., Van den Broek, H.W., and De Wit, P.J. (1994). Nitrogen limitation induces expression of the avirulence gene *avr9* in the tomato pathogen *Cladosporium fulvum*. Mol Gen Genet **243,** 277-285.

van der Does, H.C., Duyvesteijn, R.G., Goltstein, P.M., van Schie, C.C., Manders, E.M., Cornelissen, B.J., and Rep, M. (2008). Expression of effector gene *SIX1* of *Fusarium oxysporum* requires living plant cells. Fungal Genet Biol **45,** 1257-1264.

Veneault-Fourrey, C., Barooah, M., Egan, M., Wakley, G., and Talbot, N.J. (2006). Autophagic fungal cell death is necessary for infection by the rice blast fungus. Science **312,** 580-583.

Wilson, R.A., and Arst, H.N., Jr. (1998). Mutational analysis of AREA, a transcriptional activator mediating nitrogen metabolite repression in Aspergillus nidulans and a member of the "streetwise" GATA family of transcription factors. Microbiol Mol Biol Rev **62,** 586-596.

Wong, K.H., Hynes, M.J., and Davis, M.A. (2008). Recent advances in nitrogen regulation: a comparison between *Saccharomyces cerevisiae* and filamentous fungi. Eukaryot Cell **7,** 917-925.

Wong, K.H., Hynes, M.J., Todd, R.B., and Davis, M.A. (2007). Transcriptional control of *nmrA* by the bZIP transcription factor MeaB reveals a new level of nitrogen regulation in *Aspergillus nidulans*. Mol Microbiol **66,** 534-551.

Xu, J.R., and Hamer, J.E. (1996). MAP kinase and cAMP signaling regulate infection structure formation and pathogenic growth in the rice blast fungus *Magnaporthe grisea*. Genes Dev **10,** 2696-2706.

Zhao, X., Mehrabi, R., and Xu, J.R. (2007). Mitogen-activated protein kinase pathways and fungal pathogenesis. Eukaryot Cell **6,** 1701-1714.

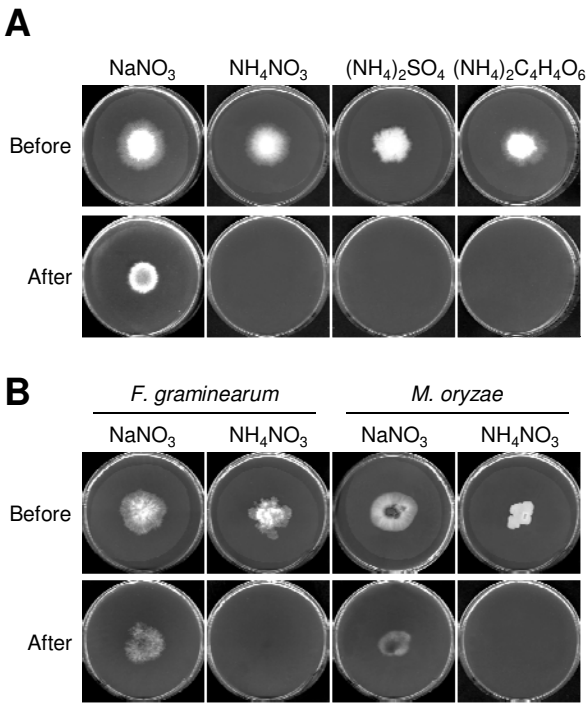

Figure 1. Nitrogen source regulates cellophane penetration in plant pathogenic fungi.
A. Effect of nitrogen source on penetration of cellophane membranes by *Fusarium oxysporum*. Fungal colonies were grown 4 days at 28ºC on plates with minimal medium containing 50 mM of the indicated nitrogen source, covered with a cellophane membrane (before). The cellophane with the fungal colony was removed and plates were incubated for an additional day to determine the presence of mycelial growth on the plate (after). **B.** Cellophane penetration of *Fusarium graminearum* and *Magnaporthe oryzae* on the indicated nitrogen source was determined as in **(A)**.

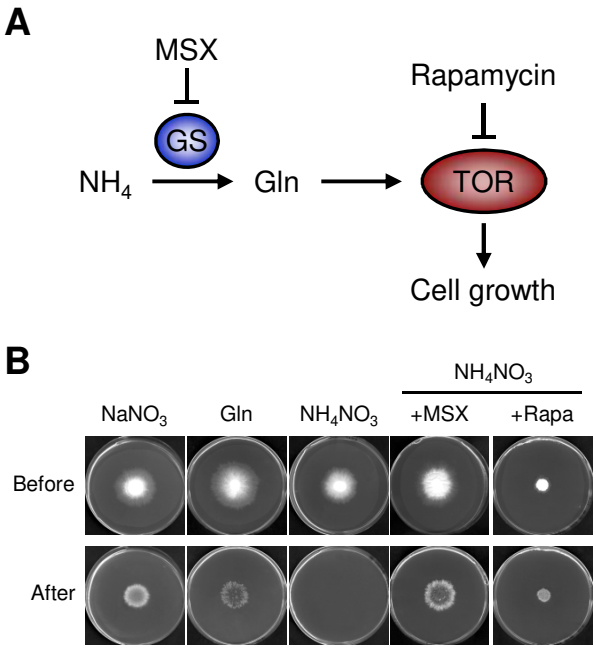

Figure 2. Ammonium repression of invasive growth is mediated by glutamine synthetase and the protein kinase TOR.
A. Model of TOR pathway activation by glutamine (adapted from Crespo *et al.* 2002). GS, glutamine synthetase; MSX, L-methionine sulfoximine. **B.** Cellophane penetration was determined on plates containing 50 mM $NaNO_3$, glutamine or NH_4NO_3 with or without 10 mM MSX, a specific inhibitor of glutamine synthetase, or 150 ng ml^{-1} rapamycin, a specific inhibitor of TOR.

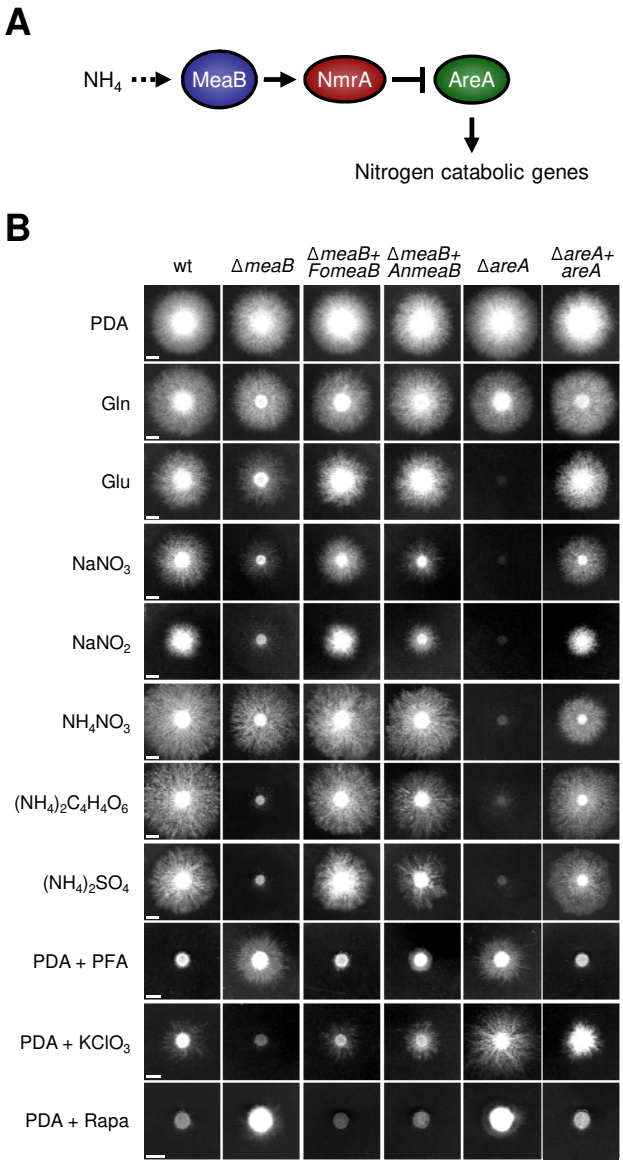

Figure 3. Effect of *meaB* and *areA* deletion on nitrogen utilization of *Fusarium oxysporum*.
A. Model of regulation of nitrogen catabolic genes in *Aspergillus nidulans* by MeaB (adapted from Wong *et al.* 2008) **B.** Growth of the indicated strains on different nitrogen sources (see Methods). Cultures were grown 3 days at 28ºC, except on NH_4NO_3, $(NH_4)_2C_4H_4O_6$, $(NH_4)_2SO_4$ and PDA + rapamycin (5 days). PDA, potato dextrose agar; PFA, DL-*p*-fluorophenylalanine. Bar 5 mm.

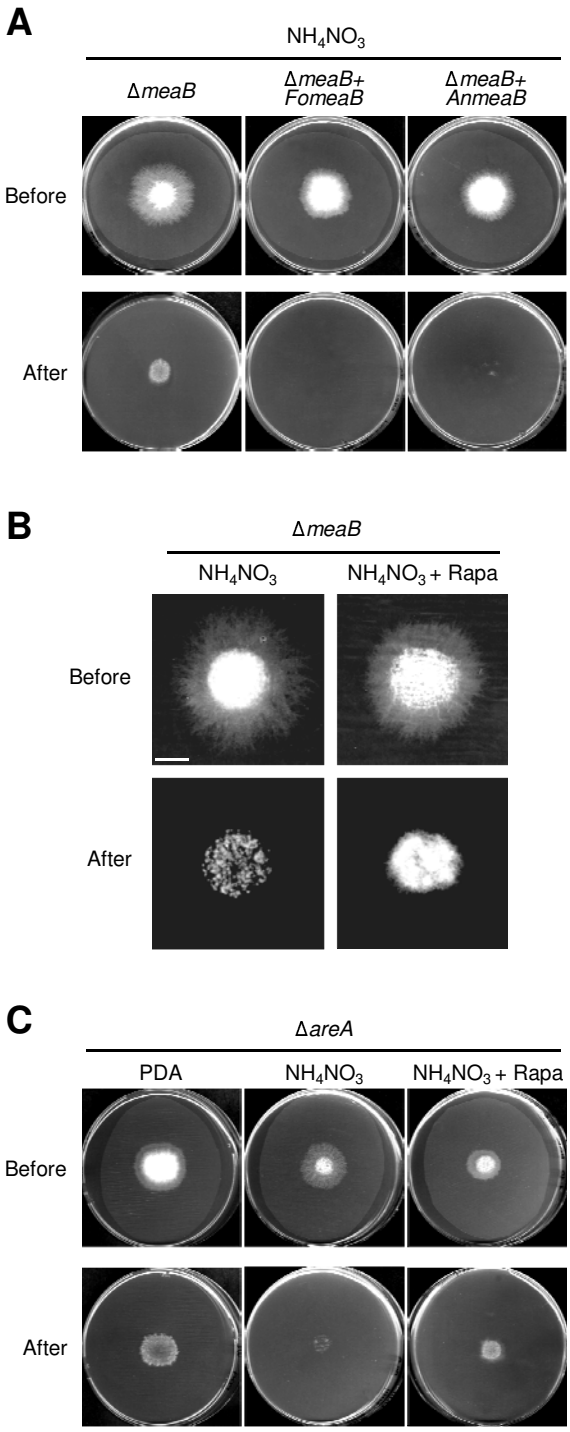

Figure 4. Ammonium repression of invasive growth is controlled by the bZIP protein MeaB and the wide domain regulator AreA.
A. Deletion of *meaB* causes invasive growth in the presence of 50 mM of the repressing nitrogen source NH_4NO_3. The indicated strains were grown 4 days before removing the cellophane membrane. **B.** MeaB and TOR have additive functions in ammonium-mediated inhibition of invasive growth. Fungal colonies were grown 3 days before removing the cellophane membrane to quantitatively compare invasion rate. Bar 5 mm. **C.** AreA is not required for invasive growth and contributes to ammonium-mediated repression of this process. Cellophane penetration of the Δ*areA* mutant was determined after 4 days incubation on plates containing PDA, or PDB diluted 1:25 with water and supplemented with 50 mM NH_4NO_3 or NH_4NO_3 + 150 ng ml^{-1} rapamycin.

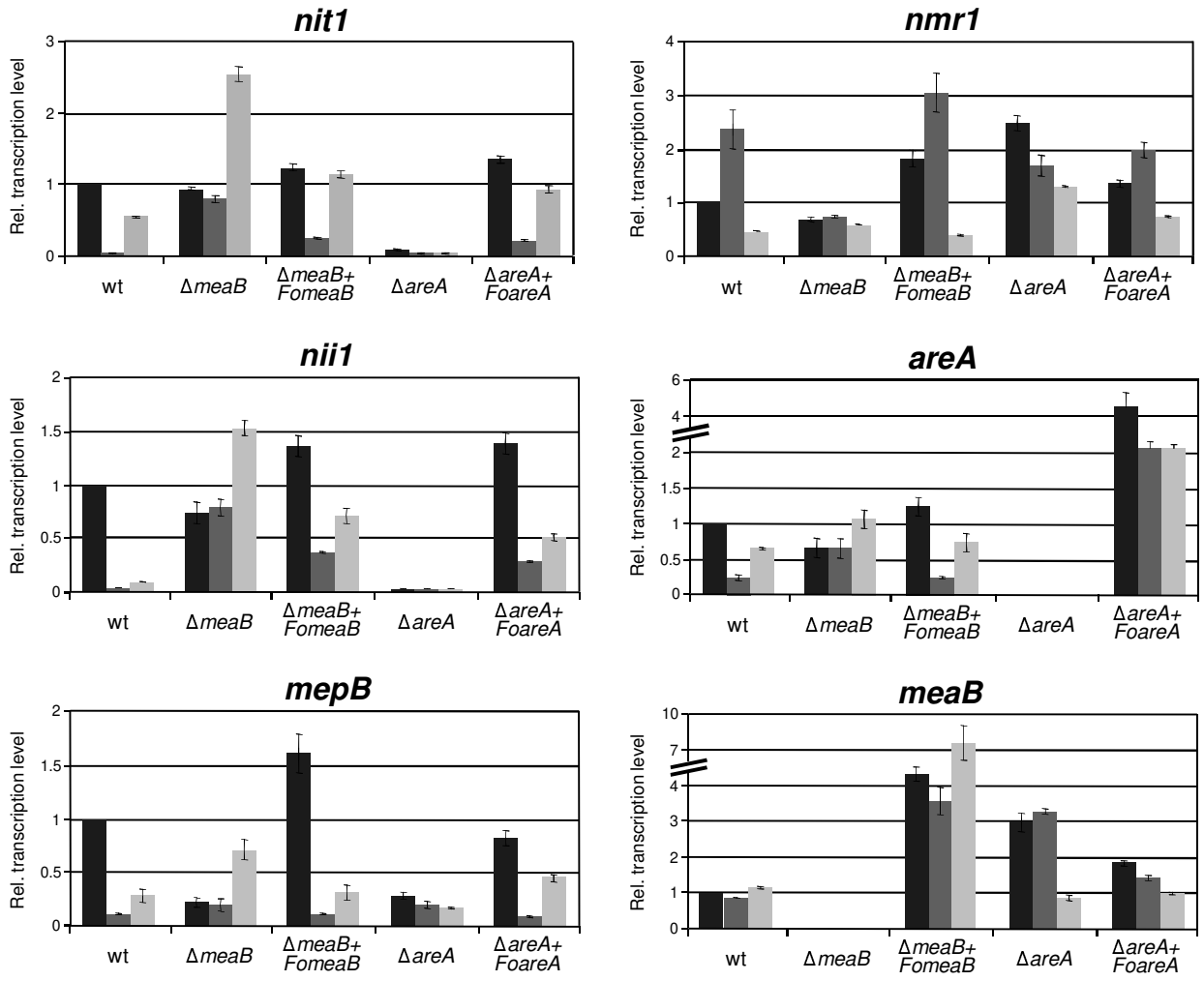

Figure 5. Effect of nitrogen source, *meaB* or *areA* deletion, and rapamycin on transcript levels of nitrogen catabolic and regulatory genes.

Quantitative real time RT-PCR analysis was performed in the indicated strains germinated 14 h in PDB diluted 1:25 with water supplemented with 25 mM $NaNO_3$, then washed with water and transferred for 3 h to 25 mM $NaNO_3$ (black columns), 25 mM NH_4NO_3 (dark grey columns) or 25 mM NH_4NO_3 + 150 ng ml^{-1} rapamycin (light grey columns) as the sole nitrogen source. Relative transcript levels represent mean ΔCt values of nitrogen catabolic genes *nit1* (nitrate reductase), *nii1* (nitrite reductase) and *mepB* (ammonium permease), as well as nitrogen regulatory genes *nmr1* (co-repressor), *areA* and *meaB*, normalized to the *act1* gene and expressed relative to transcript levels of the wild type strain on $NaNO_3$. Bars represent standard errors from 3 independent experiments with 3 replicates each.

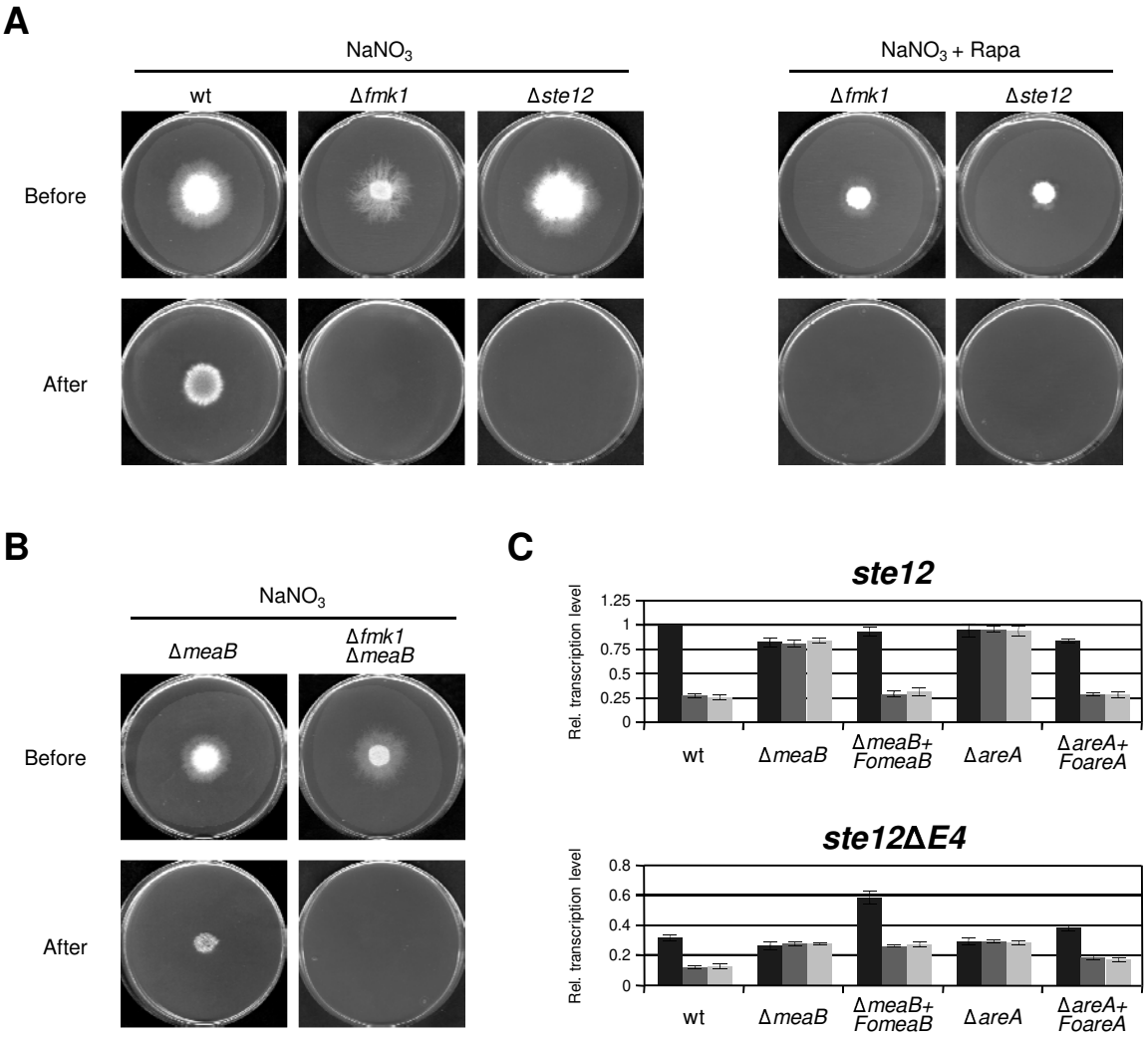

Figure 6. Inactivation of TOR or MeaB does not bypass the requirement of the Fmk1 MAPK cascade for invasive growth.

A, B. Cellophane penetration in mutants lacking the MAPK Fmk1 or the transcription factor Ste12 is not restored by 150 ng ml^{-1} rapamycin (**A**) or by *meaB* deletion (**B**). **C.** Expression of *ste12* is repressed by nitrogen source via MeaB and AreA. Quantitative real time RT-PCR analysis was performed in the indicated strains germinated as described in Figure 5 and transferred for 3 h to $NaNO_3$ (black columns), NH_4NO_3 (dark grey columns) or NH_4NO_3 + 150 ng ml^{-1} rapamycin (light grey columns) as the sole nitrogen source. Relative transcript levels represent mean ΔCt values of differentially spliced transcripts *ste12* (containing the five predicted exons) and *ste12ΔE4* (lacking exon 4), normalized to *act1* and expressed relative to transcript levels of *ste12* in the wild type strain on $NaNO_3$. Bars represent standard errors from 3 independent experiments with 3 replicates each.

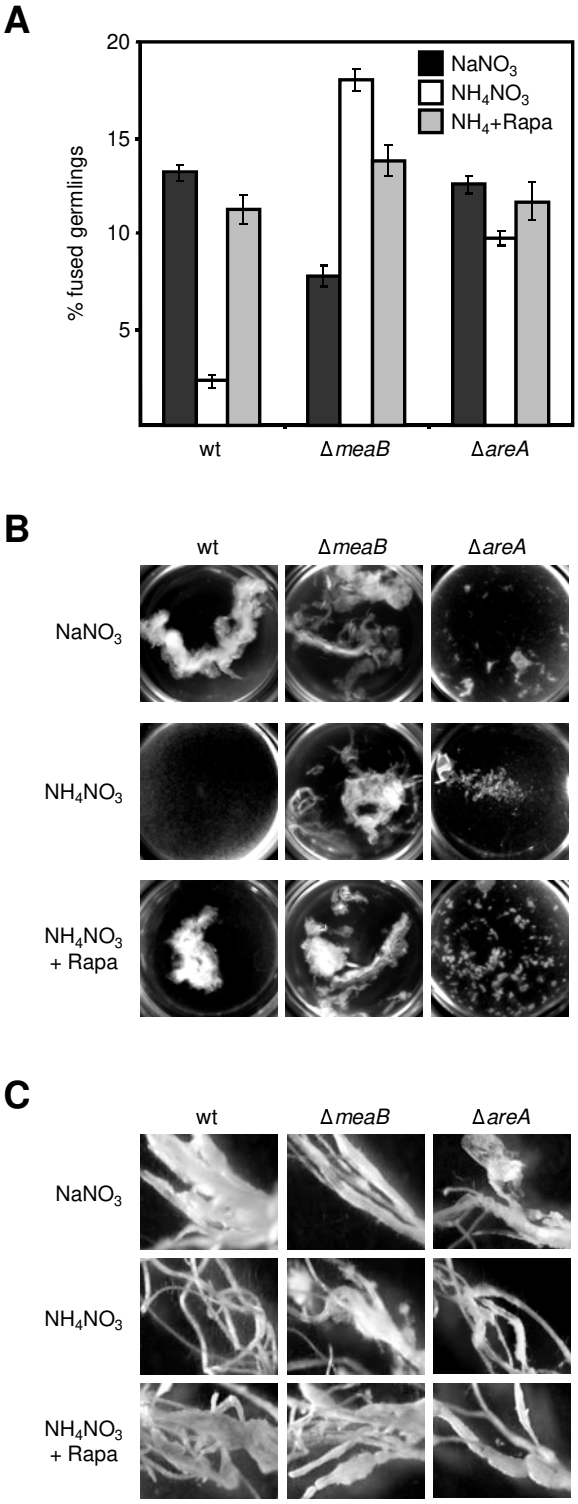

Figure 7. Nitrogen source regulates vegetative hyphal fusion, hyphal aggregation and root adhesion via TOR and MeaB.

A. Frequency of vegetative hyphal fusion of the indicated strains after 18 h of conidial germination in PDB diluted 1:25 with water and supplemented with 25 mM of the indicated nitrogen source was determined microscopically and expressed as percentage of fused germlings versus total number of germlings. Bars represent standard errors from 3 independent experiments with 3 replicates each. **B.** Hyphal aggregates forming after 36 h conidial germination under conditions described in (**A**). Cultures were vortexed to dissociate weakly adhered hyphae and observed in a binocular microscope. **C.** Root adhesion assay. Roots of tomato seedlings were immersed for 36 h in microconidial suspensions of the indicated strains in PDB diluted 1:25 with water and supplemented with 25 mM of the indicated nitrogen source, then washed by vigorous shaking in water and observed in a binocular microscope. Adhering fungal mycelium is visible as a white mass covering the roots.

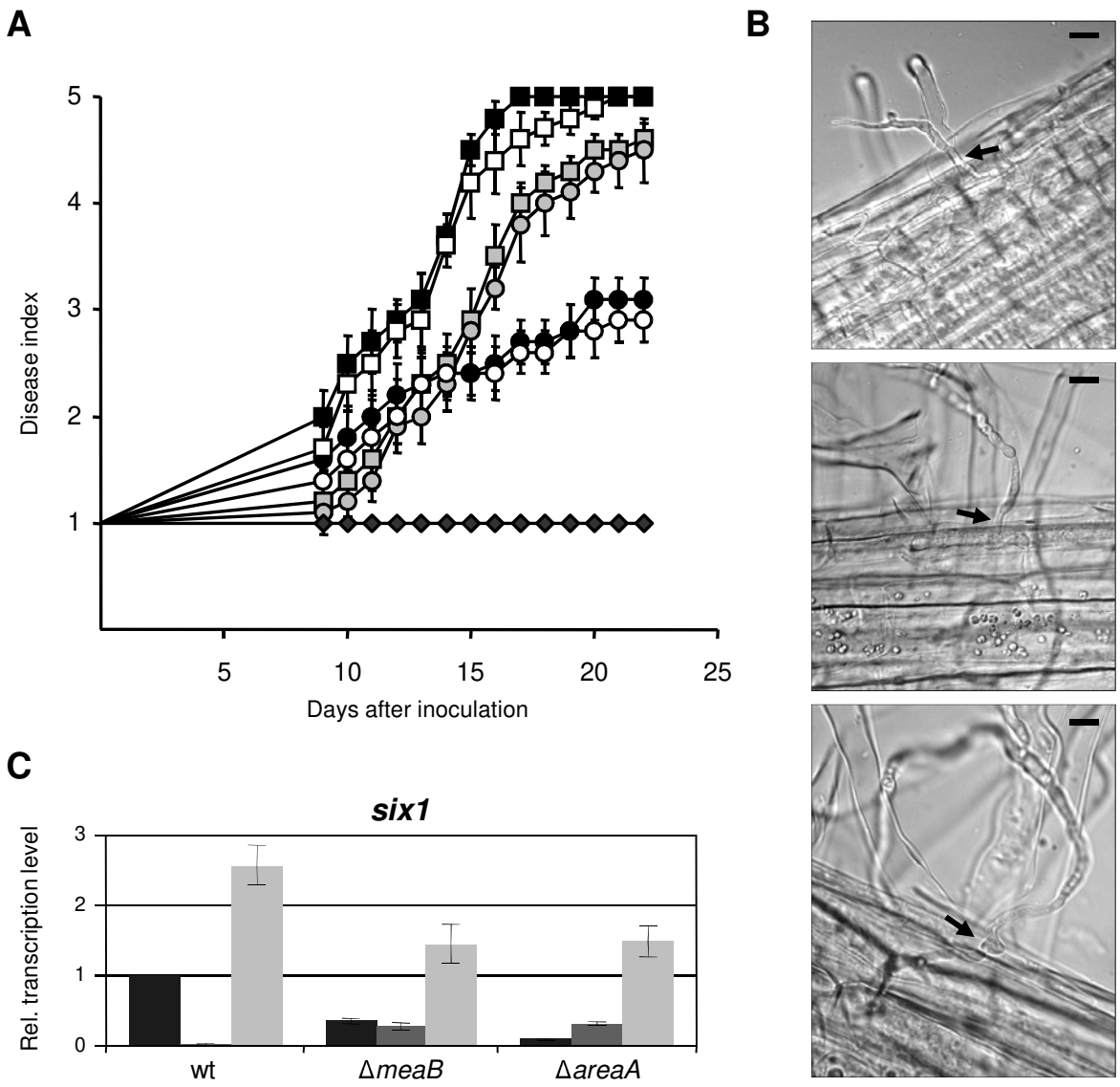

Figure 8. Nitrogen source and MeaB control infection of tomato plants.
A. Incidence of *Fusarium* wilt on tomato plants (cultivar Monica) inoculated with the wild type strain (black symbols), the Δ*meaB* mutant (grey symbols) and the Δ*meaB + FomeaB* complemented strain (white symbols). Plants were supplied either with 25 mM $NaNO_3$ (squares) or 25 mM NH_4NO_3 (circles) solutions in water. Uninoculated plants supplied with 25 mM $NaNO_3$ (dark grey diamonds) were used as controls. Severity of disease symptoms was recorded at the indicated times using an index ranging from 1 (healthy plant) to 5 (dead plant). Bars represent standard errors calculated from 10 plants. **B.** Penetration of tomato roots by infection hyphae of *F. oxysporum.* Roots of tomato seedlings were immersed for 24 h in a microconidial suspension of the wild type strain in the presence of 25 mM $NaNO_3$ and observed microscopically. Arrows point to sites of penetration. Bar 10 µm. **C.** Quantitative real time RT-PCR analysis of the plant-induced virulence effector gene *six1* in different *F. oxysporum* strains 48 h after inoculation on tomato roots supplied with 25 mM $NaNO_3$ (black columns), 25 mM NH_4NO_3 (dark grey columns) or 25 mM NH_4NO_3 + 150 ng ml^{-1} rapamycin (light grey columns) as the sole nitrogen source. Relative transcript levels represent mean ΔCt values of *six1* normalized to *act1* and expressed relative to transcript levels of the wild type strain on $NaNO_3$. Bars represent standard errors from 3 independent experiments with 3 replicates each.

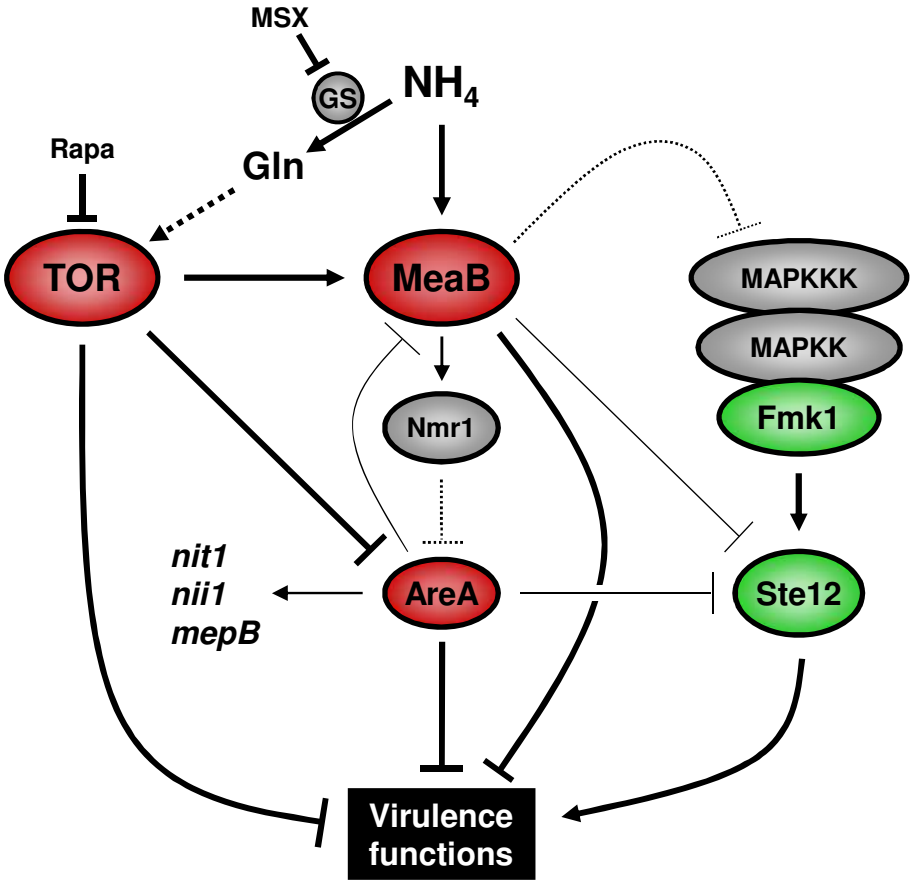

Figure 9. Nitrogen controls virulence functions in *Fusarium oxysporum* through TOR and MeaB. The preferred nitrogen source ammonium represses virulence functions via glutamine synthetase, the protein kinase TOR, the bZIP protein MeaB and the GATA factor AreA. Thick lines indicate results based on genetic or pharmacological evidence, thin lines indicate results based on expression analysis. Ammonium depletion, MSX or rapamycin lead to inactivation of TOR and/or MeaB, thus promoting virulence functions. TOR mediates repression of nitrogen catabolic genes and virulence functions both by MeaB-dependent and independent mechanisms. AreA has a dual role as an activator of nitrogen catabolic genes and as a repressor of virulence functions. The MAPK Fmk1 and the downstream homeodomain transcription factor Ste12 are required for activation of virulence functions through a positive regulatory pathway. Ammonium represses *ste12* expression through MeaB and AreA. A possible role of the nitrogen repression pathway upstream of Fmk1 cannot be excluded.

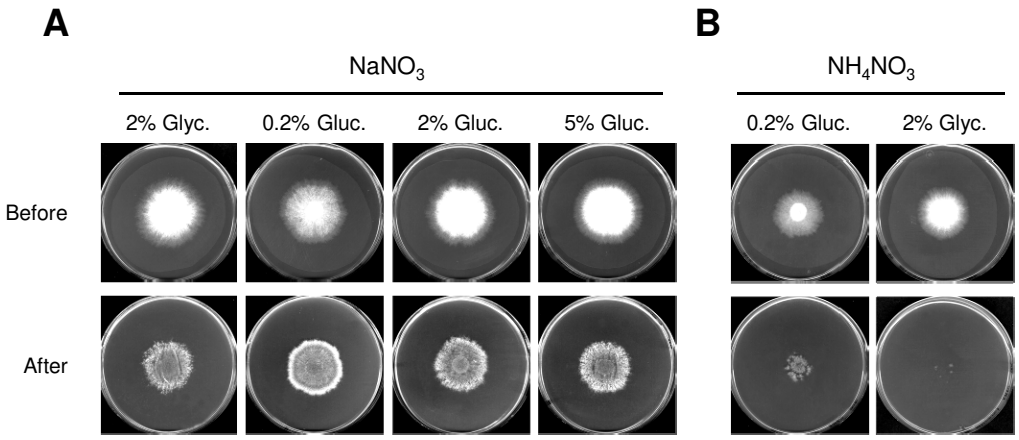

Supplemental Figure 1. Effect of carbon source on cellophane penetration by *Fusarium oxysporum*. Cellophane penetration on minimal medium containing 50 mM $NaNO_3$ or NH_4NO_3 as a nitrogen source and the indicated carbon sources.

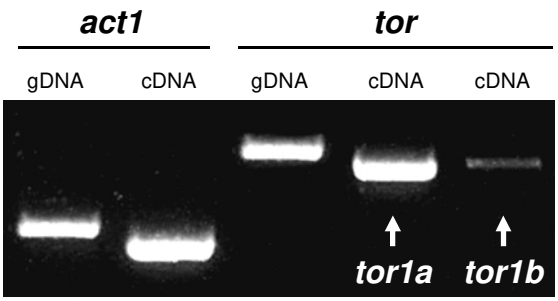

Supplemental Figure 2. Expression of *Fusarium oxysporum tor1a* and *tor1b* genes.
Transcripts of *tor1a* and *tor1b* were detected by RT-PCR (40 cycles) in the wild type strain germinated 14 h in PDB, washed in water and transferred for 3 h to liquid minimal medium containing 25 mM NH_4NO_3 as the nitrogen source.

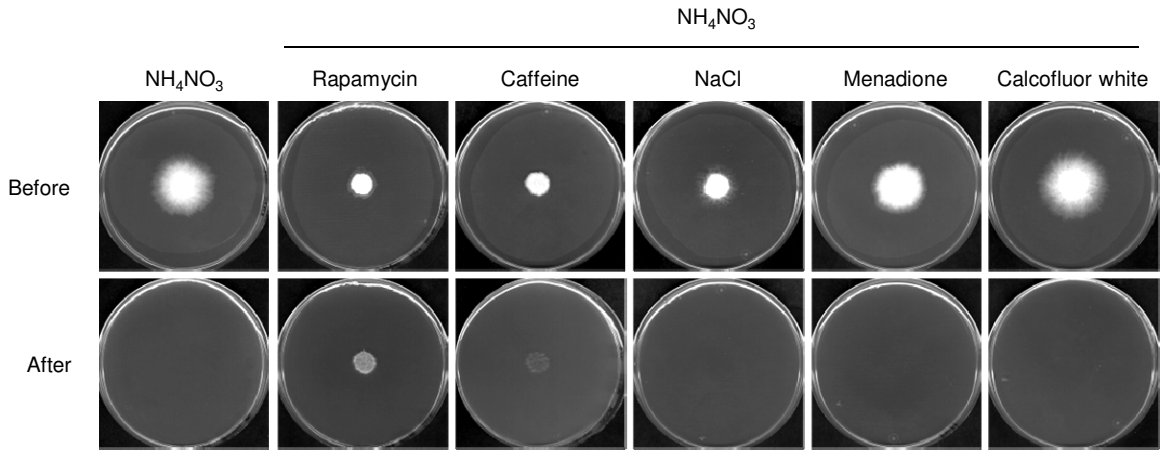

Supplemental Figure 3. Cellophane penetration on ammonium is specifically induced by TOR inhibition, but not by salt, oxidative or cell wall stress.
Cellophane penetration was determined on plates containing 50 mM NH_4NO_3 in the presence or absence of 150 ng ml^{-1} rapamycin, 10 mM caffeine, 0.8 M NaCl, 10 µg ml^{-1} menadione or 20 µg ml^{-1} calcofluor white.

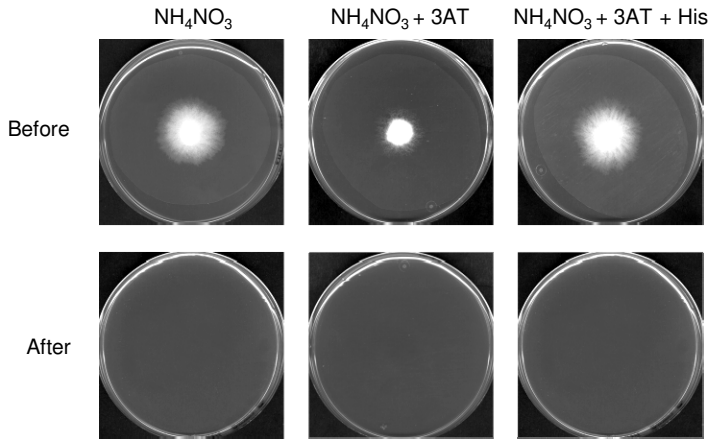

Supplemental Figure 4. Nitrogen regulation of invasive growth is not mediated by the general amino acid control system.
Cellophane penetration was determined on plates containing 50 mM NH_4NO_3 in the presence or absence of 10 mM 3-amino-triazole (3AT), a histidine-analogue that induces histidine starvation, or 3AT + 1 mM histidine.

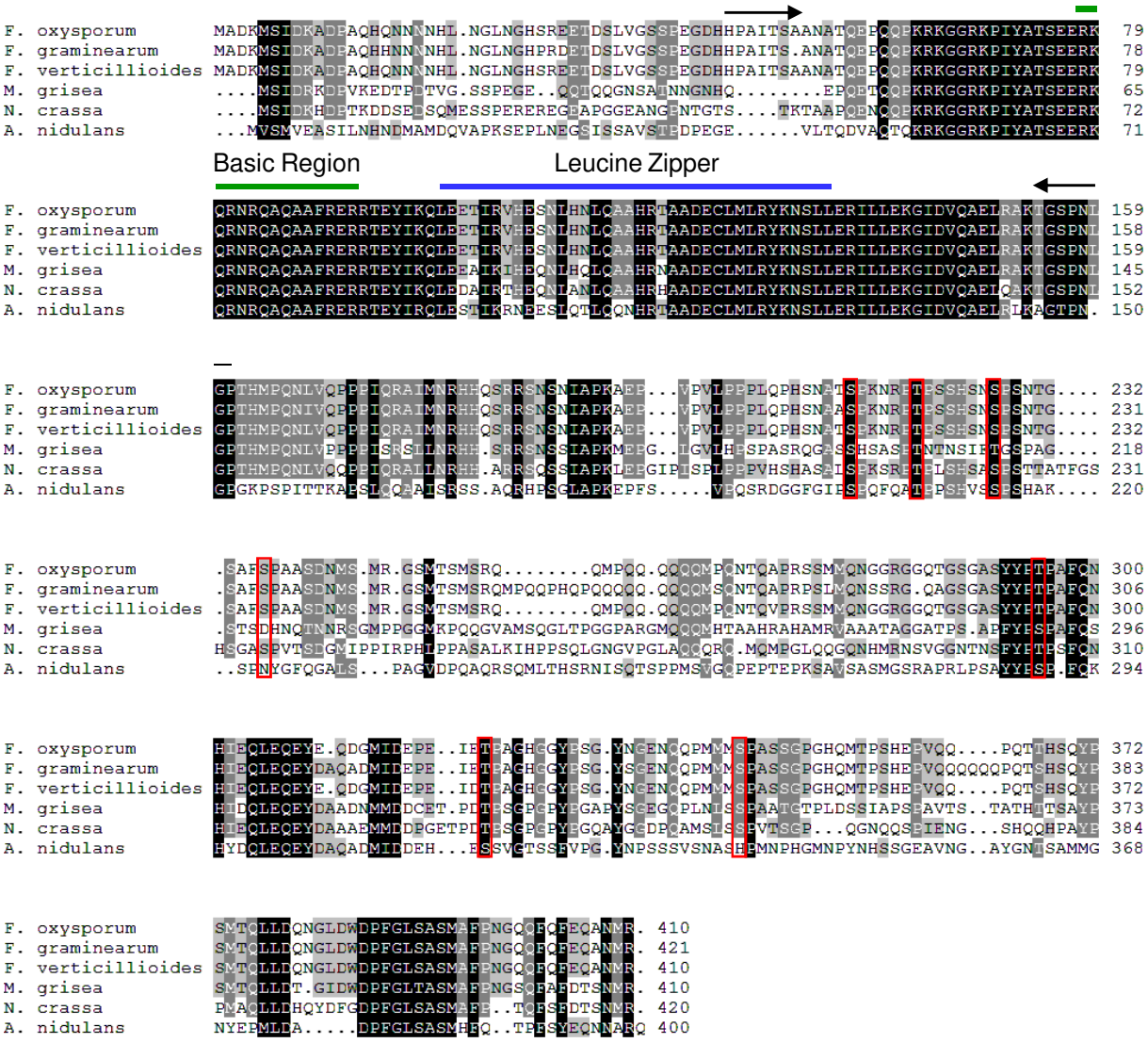

Supplemental Figure 5. Amino acid sequence alignment of fungal orthologues of the bZIP protein MeaB. The predicted *Fusarium oxysporum meaB* gene product (FOXG_02277) was aligned with MeaB proteins from *Fusarium graminearum* (XP_3836840), *Fusarium verticillioides* (FVEG_05452), *Magnaporthe grisea* (XP_359471), *Neurospora crassa* (XP_957694) and *Aspergillus nidulans* (CAA74033). Absolutely conserved residues are shaded in black, residues conserved in at least 80% are shaded in dark gray and residues conserved in at least 60% are shaded in light gray. The basic region and leucine zipper domains (Wong et al. 2007) are indicated by a green and blue line, respectively. Black arrows indicate the relative positions of the primers used for qRT/PCR. Conserved serine and threonine residues followed by a proline, which resemble the rapamycin-sensitive phosphorylation sites in TOR-regulated yeast protein kinases are marked by red boxes.

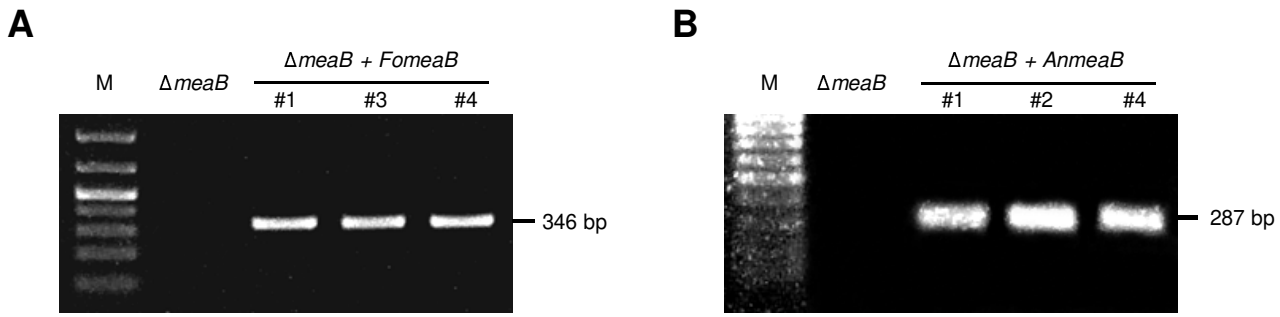

Supplemental Figure 6. Complementation of the *Fusarium oxysporum meaB* deletion mutant with *FomeaB* or *AnmeaB*.

PCR amplification of genomic DNA of the Δ*meaB strain* and three independent complemented transformants with primer pairs 6G5-5 + 6G5-6 (**A**) or AnmeaB-1 + AnmeaB-2 (**B**). The complemented strains produce banding patterns consistent with the integration of an intact *FomeaB* **(A)** or *AnmeaB* **(B)** gene.

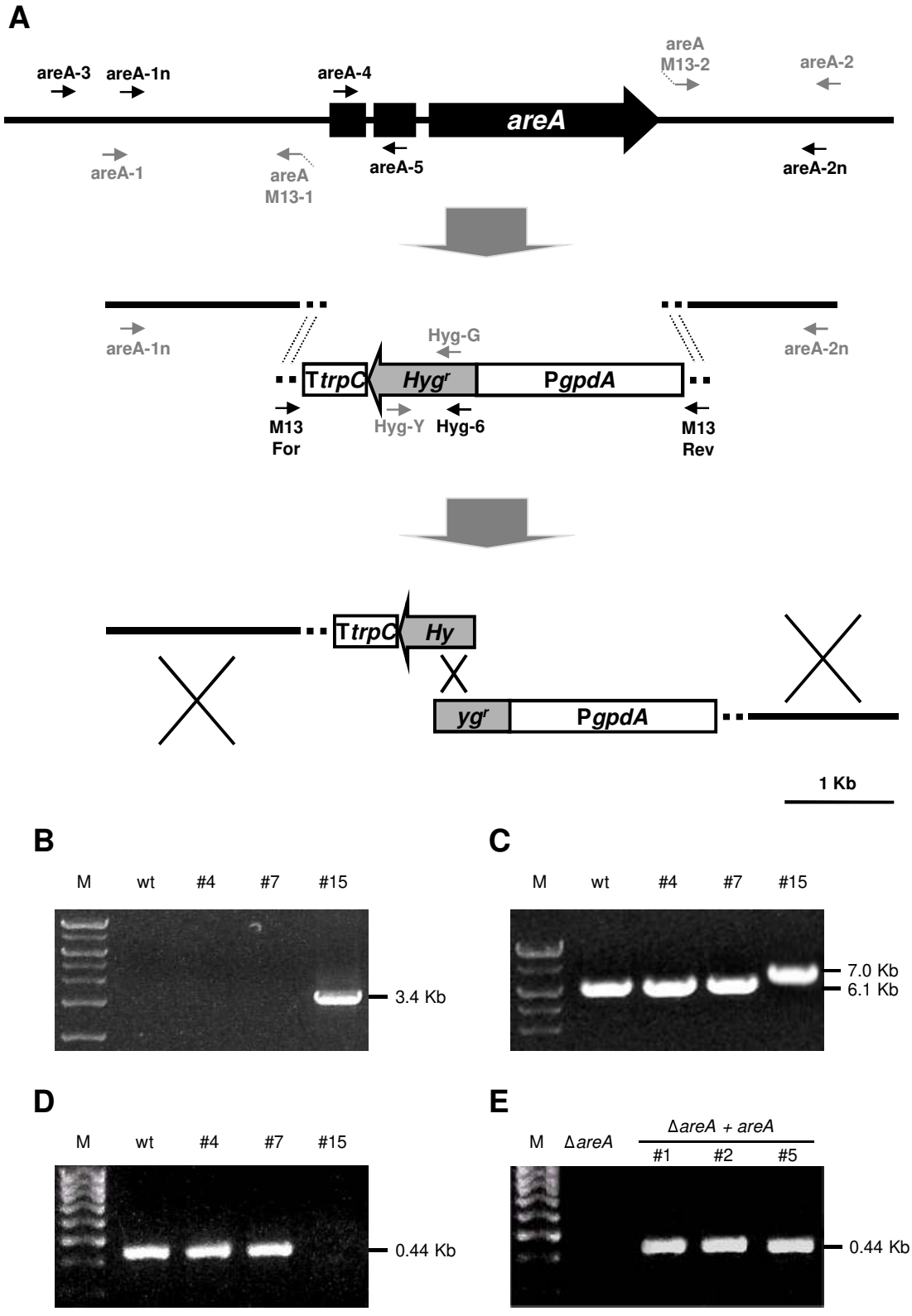

Supplemental Figure 7. Targeted deletion of the *Fusarium oxysporum areA* gene.
A. Physical maps of the *F. oxysporum areA* locus and of the split-marker gene replacement constructs obtained by fusion PCR. Primers used in each PCR step are shaded in grey. **B-D.** PCR amplification of genomic DNA of the wild type strain and three independent transformants, using primer pairs areA-3 + hyg-6 (**B**), areA-1n + areA-2n (**C**) or areA-4 + areA-5 (**D**). Transformant #15 produces a banding pattern consistent with homologous replacement of the *areA* gene. **E.** PCR amplification of genomic DNA of the Δ*areA strain* and three independent complemented transformants, using primer pair areA-5 + areA-6. All complemented strains produce a banding pattern consistent with the integration of an intact *areA* gene.

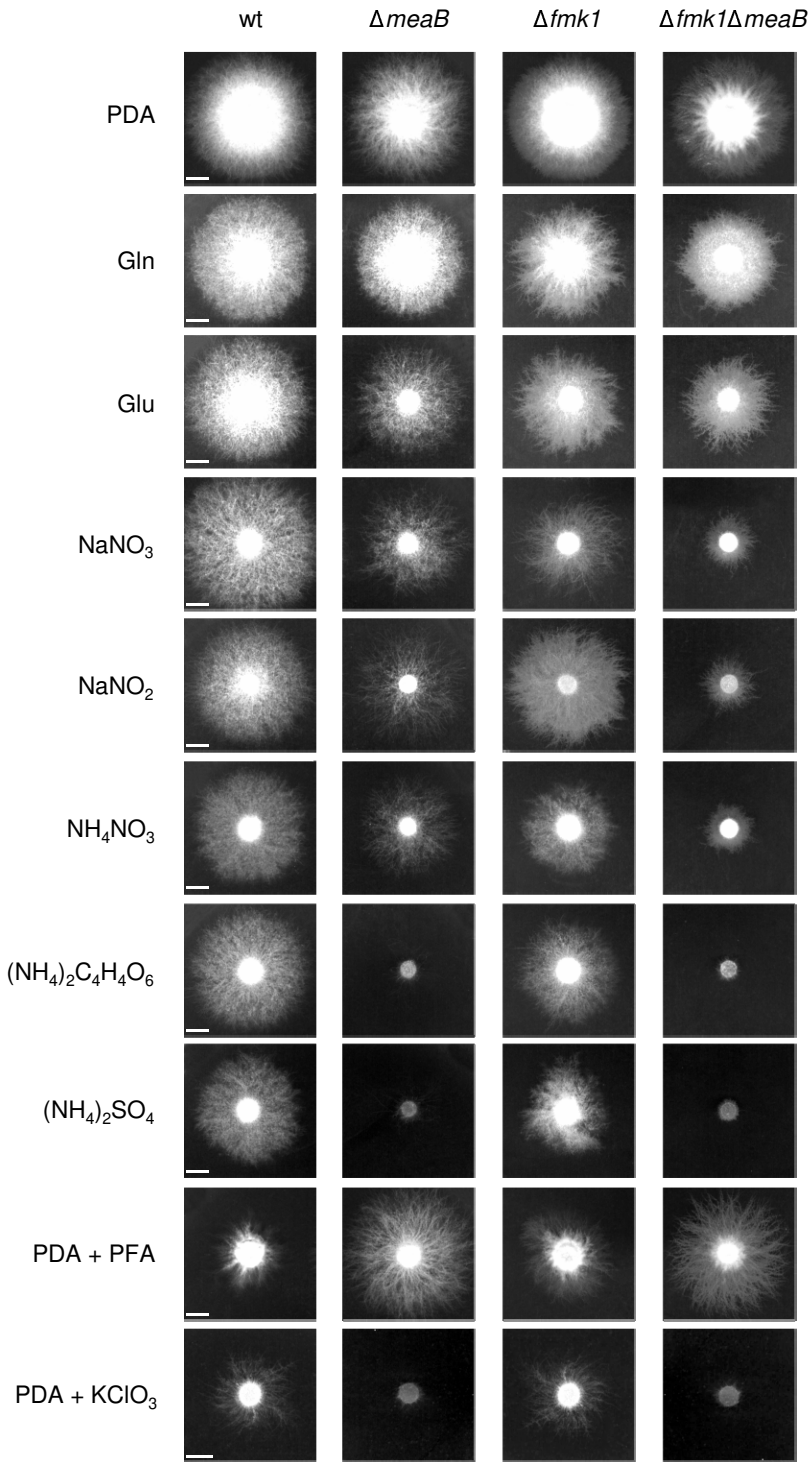

Supplemental Figure 8. Nitrogen utilization phenotypes caused by single and double deletion of *meaB* and *fmk1*.

Growth of the indicated strains on minimal medium supplemented with different nitrogen sources (see methods) was determined after 4 days at 28ºC, except on PDA, Gln and Glu (3 days). PDA, potato dextrose agar; PFA, DL-*p*-fluorophenylalanine. Bar 5 mm.

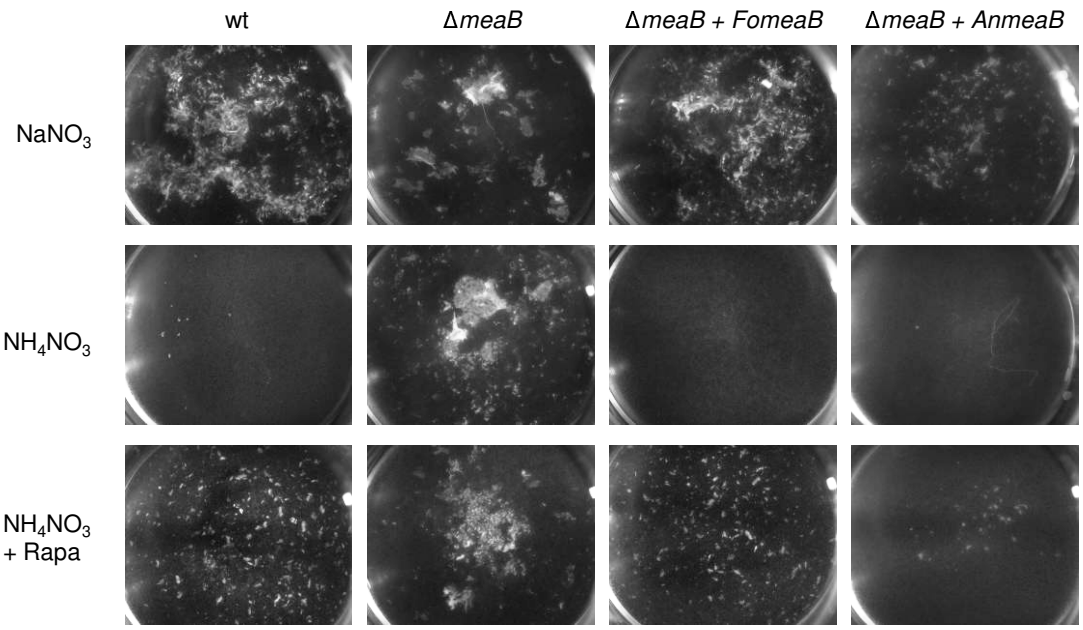

Supplemental Figure 9. Nitrogen source regulates hyphal aggregation via TOR and MeaB.
Hyphal aggregation of the indicated stains after 24 h of conidial germination in PDB diluted 1:25 with water and supplemented with 25 mM of the indicated nitrogen source. Cultures were vortexed to dissociate weakly adhered hyphae and observed in a binocular microscope.

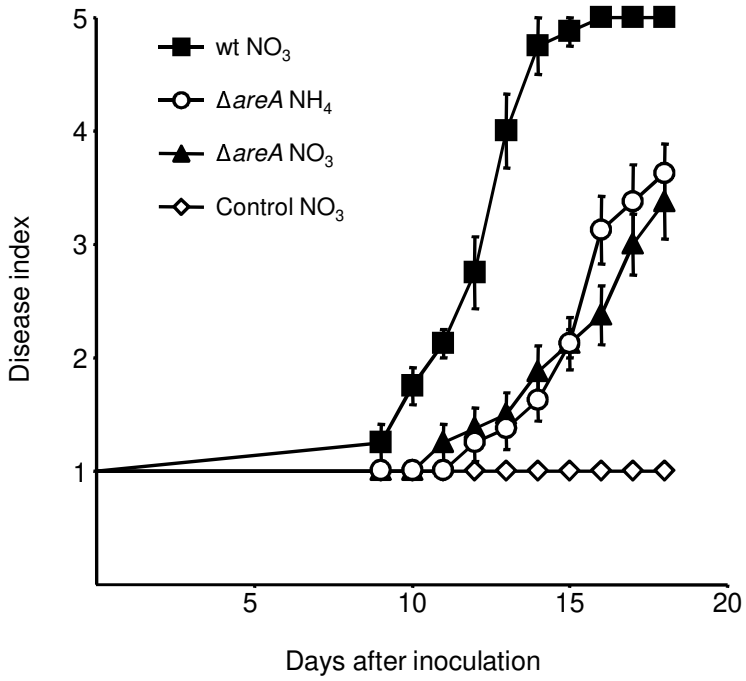

Supplemental Figure 10. AreA contributes to virulence of *Fusarium oxysporum* on tomato plants independently of nitrogen source.
Incidence of *Fusarium* wilt on tomato plants (cultivar Monica) inoculated with the wild type strain or the Δ*areA* mutant. Plants were supplied with 25 mM of the indicated nitrogen source. Control refers to uninoculated plants. Severity of disease symptoms was recorded using an index ranging from 1 (healthy plant) to 5 (dead plant). Bars represent standard errors calculated from 10 plants.

Supplementary Table 1. List of primers used in this study

Use		Primer	Sequence (5'→3')
Tor sequencing		tor1a-For	CTGTAACACCCTCCTCGCCC
		tor1a-Rev	GGCTGTGTCGCGATCAGAGTT
		tor1b-For	CTATGCAATACCCTTCTGGCTT
		tor1b-Rev	CTGCGTCTCTGTCGGAGCG
Knockout *areA*		areA-1	GGTTCAGACAAAGGCAAAGTTC
		areA-2	TTTGCCGAAGTTGAATGGGATG
		areA-3	GAGGTATGAGGGGAAAAACAG
		areA-1n	TGAATGCTCGTCCCTGCTCC
		areA-2n	ACTCGGAAACTGATGCGGGC
		areA-M13-1	GTGACTGGGAAAACCCTGGCGAAGTGGGAGCGTTGTGAATAG
		areA-M13-2	TCCTGTGTGAAATTGTTATCCGCTAGATACCTTACTTGGATGTGTTA
qRT-PCR	*act1*	act-2	GAGGGACCGCTCTCGTCGT
		act-q6	GGAGATCCAGACTGCCGCTCAG
	nit1	nit1-For	CGGCTACTGGGGTGAGAAGG
		nit1-Rev	GGAACACTTCTCGGTCTGCG
	nii1	nii1-For	TGTTGCTGGTGGTATGGAGTC
		nii1-Rev	TCGCACCACCGTTACCGCC
	mepB	mepB-1	CCTCTCTGCTAACCTTCGTG
		mepB-2	CGAGACTGTAACCATCAAAGAC
	nmr1	nmr1-1	TTTCACCTCCCTTCAGTATCC
		nmr1-2	GACCATTTGCTTCCTCTTCTAT
	areA	areA-4	AGAGCAGCAGCAGAGGCAAG
		areA-5	CTGGTGAACTGGCTGGACGG
	meaB	6G5-5	CCCTGCGATAACCTCTGCTG
		6G5-6	GTTCCTCTGCTTTCGCTCTTC
	six1	six1-1	ATAGCATGGTACTCCTTGGCG
		six1-2	CCTGATGGTGACGGTTACGAA
	ste12	ste12-For	CCGCTCTGTTCCTGCTCCCA
		ste12-Rev	GCAGTGGGGACAGATGTAAGG
		ste12ΔE4-Rev	TACGCTTGTGTCGCTTGAGATG
***meaB* complementing**		AnmeaB-For	GACGCTGCTTTGGGATTGACT
		AnmeaB-Rev	GGGGGAAGGCTCTCTGTTAT
		FomeaB-For	AGTGACCTGGCGGCGTACCT
		FomeaB-Rev	CAAAAGATGGTATTCACTGCGT
		AnmeaB-1	TGAATGCTTGATGCTGCGTTAC
		AnmeaB-2	GACTGGGGAACACTGAAAGG
***hyg*B cassette**		M13-For	CGCCAGGGTTTTCCCAGTCACGAC
		M13-Rev	AGCGGATAACAATTTCACACAGGA
		hyg-6	TCGTTATGTTTATCGGCACTTT
		hyg-Y	GGATGCCTCCGCTCGAAGTA
		hyg-G	CGTTGCAAGACCTGCCTGAA